Great earthquakes on Canada's west coast: a review [1,2]

Roy D. Hyndman and Garry C. Rogers

Abstract: The first Lithoprobe transect in 1984 across Vancouver Island had primary objectives to define the structure associated with subduction and constraints on the potential for great thrust earthquakes. The Lithoprobe results and the comprehensive multidisciplinary data collection and analyses that followed provide compelling evidence for past great earthquakes along the Cascadia subduction zone from Vancouver Island to northernmost California, and for present elastic strain build up toward future great events. There is evidence of sudden coastal subsidence up to 2 m and of deep-sea turbidite deposits indicating strong shaking from huge earthquakes at irregular intervals averaging about 500 years, the last in 1700. Precision geodetic measurements define the present buckling of the coastal region, diagnostic of elastic strain accumulation on a locked thrust fault. The landward extent of rupture and, therefore, shaking at coastal cities is constrained by (*i*) the pattern of elastic strain buildup, (*ii*) the estimated temperatures on the fault, (*iii*) the updip limit of episodic tremor and slip (ETS), (*iv*) the downdip change in reflection character of the thrust, and (*v*) the magnitude of coastal subsidence in the most recent, 1700, and previous great events. The major earthquakes are very large, M9, rupturing most of the Cascadia margin, but mainly offshore, limiting somewhat the shaking at inland cities but producing large tsunamis. The ETS that occurs at intervals of just over a year appears to involve slow slip on the subduction thrust downdip of the rupture zone that increases stress on the locked zone and may indicate time varying potential for great events.

Résumé : Les principaux objectifs du premier transect Lithoprobe traversant l'île de Vancouver en 1984 étaient de définir la structure associée à la subduction et les contraintes sur le potentiel de grands tremblements de terre par chevauchement. Les résultats Lithoprobe, et la collecte et l'analyse des très vastes données multidisciplinaires qui en ont découlé, fournissent des évidences convaincantes pour d'anciens grands tremblements de terre le long de la zone de subduction Cascadia, de l'île de Vancouver à l'extrémité nord de la Californie, et pour l'actuelle contrainte de déformation élastique qui s'accumule pour causer de futurs grands événements. Il existe des preuves d'une soudaine subsidence de la côte atteignant 2 m et la déposition de dépôts de turbidites dans les grands fonds océaniques, ce qui indique de fortes secousses de grands tremblements de terre à des intervalles irréguliers, d'une moyenne d'environ 500 ans, le dernier ayant eu lieu en 1700. Des mesures géodésiques précises définissent le flambage actuels de la région de la côte, diagnostiquant une accumulation de contraintes de déformation élastique sur une faille chevauchante figée. L'étendue de rupture vers le continent, et donc le tremblement aux villes côtières, est limitée par (*i*) les tendances d'accumulations de contraintes de déformation élastique, (*ii*) la température estimée de la faille, (*iii*) la limite en amont-pendage de trémors et de glissements épisodiques (TGÉ), (*iv*) le changement en aval-pendage du caractère de réflexion du chevauchement et (*v*) la magnitude de la subsidence côtière lors des grands évé nements les plus récent, ceux de 1700 et les anciens. La plupart des principaux tremblements de terre sont très gros, M9, brisant la plus grande partie de la bordure Cascadia surtout; cependant, au large, limitant quelque peu le tremblement aux villes internes mais produisant de grands tsunamis. Les TGÉ qui se produisent à des intervalles légèrement supérieurs à un an semblent impliquer un glissement lent sur le chevauchement de la subduction en aval-pendage de la zone de rupture, ce qui augmente progressivement les contraintes sur la zone figée; ils pourraient aussi indiquer un potentiel, variable dans le temps, pour de grands événements.

[Traduit par la Rédaction]

Received 27 August 2009. Accepted 2 February 2010. Published on the NRC Research Press Web site at cjes.nrc.ca on 8 June 2010.

Paper handled by Associate Editor R. Clowes.

R.D. Hyndman[3] and G.C. Rogers. Pacific Geoscience Centre, Geological Survey of Canada, 9860 W. Saanich Road, P.O. Box 6000, Sidney, BC V8L 4B2, Canada.

[1]This article is one of a series of papers published in this Special Issue on the theme *Lithoprobe — parameters, processes, and the evolution of a continent*.
[2]Geological Survey of Canada Contribution 20090196.
[3]Corresponding author (e-mail: rhyndman@nrcan.gc.ca).

Introduction

It is well recognized that the coast of British Columbia and the US Pacific Northwest has substantial earthquake hazard. In the past 100 years, there was an M = 8.1 strike-slip event on the coast of the Queen Charlotte Islands in 1949 (e.g., Rogers 1986), two major (M $\sim$ 7) earthquakes causing damage on Vancouver Island in 1918 and 1946 (e.g., Milne et al. 1978; Rogers and Horner 1991; Rogers and Hasegawa 1978; Cassidy et al. 1988; Rogers 1998) and in Washington State damaging Wadati-Benioff earthquakes at a depth of about 60 km beneath Puget Sound in 1949 and 1965, and most recently in 2001 (Rogers et al. 1996;

Fig. 1. Main Lithoprobe corridor, with summary of historical earthquakes in the region and the most recent, 1700, megathrust earthquake. Stars, M > 6.5; circles, M > 3.

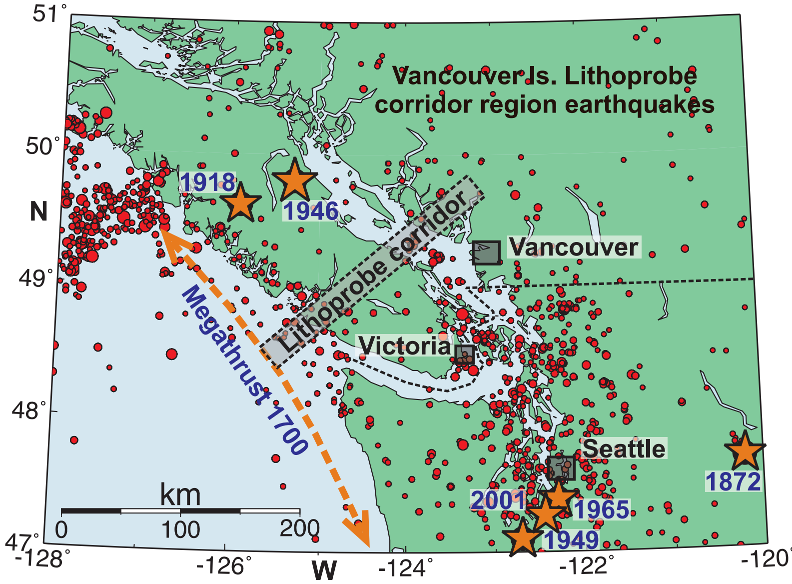

Fig. 2. Schematic cross-section of the Cascadia subduction and megathrust earthquake zone and the epicentres of some larger historical earthquakes (stars).

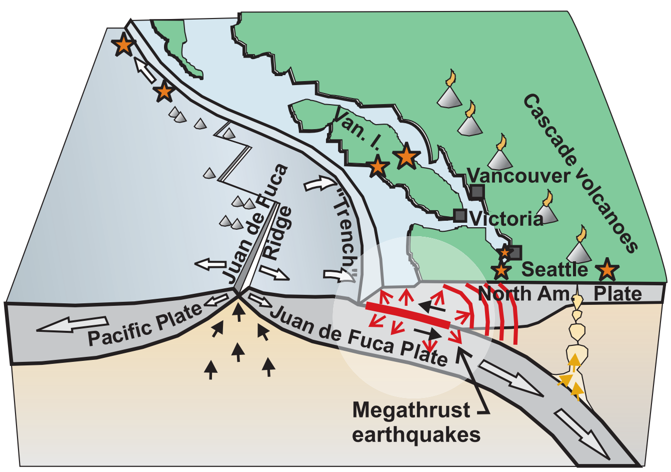

Preston et al. 2003; Rogers and Crosson 2002) (Fig. 1). However, until the mid 1980s the risk of great subduction thrust events was not appreciated (Fig. 2) because there had been no giant earthquakes of the type characteristic of convergent margins in the written historical record. It was even questioned whether there was current subduction because there is no clear trench and there was only limited historical arc volcanism. The evidence that there is indeed active subduction underthrusting was summarized by Riddihough and Hyndman (1976), and the case for great earthquakes was made more than 20 years ago (e.g., Heaton and Kanamori 1984; Heaton and Hartzell 1986, 1987; Rogers 1988), although supporting data were limited. In the past 20 years, however, the accumulated evidence has left little doubt that great earthquakes and associated tsunamis have occurred many times in the past and that they will occur and produce damage in the future.

In this review article for Lithoprobe-related studies, we emphasize data and analyses from the Vancouver Island portion of the Cascadia margin, but include information on the whole subduction zone from Vancouver Island to northernmost California. Previous summaries have been provided by Clague et al. (1995), Hyndman (1995*a*), Hyndman et al. (1996), and Clague and Bobrowsky (1999). The initial Lithoprobe study was deep crustal-scale multichannel seismic reflection across the middle of Vancouver Island to define the subduction zone structure (Yorath et al. 1985; Green et al. 1986; Clowes et al. 1987*a*; Clowes and Hyndman 2002). That study provided a focus for many additional studies. A major strength of the subsequent work has been the concentration of multidisciplinary studies in this Vancouver Island Lithoprobe corridor, its offshore extension, and inland extension into the Coast Mountains. The initial Lithoprobe land study was followed by marine multichannel reflection across the margin from the deep sea to the coast (Clowes et al. 1987*b*; Davis and Hyndman 1989; Hyndman et al. 1990, 1995*b*, and references therein) and the SHIPS (Seismic Hazards Investigation of Puget Sound) program in Georgia Strait and Puget Sound (Fisher et al. 1999; Brocher et al. 2001; Ramachandran et al. 2005, 2006). There also were large-scale seismic refraction experiments (Spence et al. 1985; Spence et al. 1991; Graindorge et al. 2003). Other studies included seismic tomography, seismic receiver function structure, seismicity, gravity, magnetics, magnetotellurics, heat flow, seafloor sampling and mapping in the offshore, and detailed surface geology across Vancouver Island (e.g., Yorath et al. 1999). There also have been two programs of international ocean drilling near the corridor (Ocean Drilling Program/Integrated ODP (ODP/IODP) 146/311) justified in part by the extensive concentration of multidisciplinary studies characterizing the tectonic environment.

Earthquake statistics and seismic hazard in the region

The earthquake hazard in a region is generally estimated

Fig. 3. The three earthquake types of the Cascadia subduction zone.

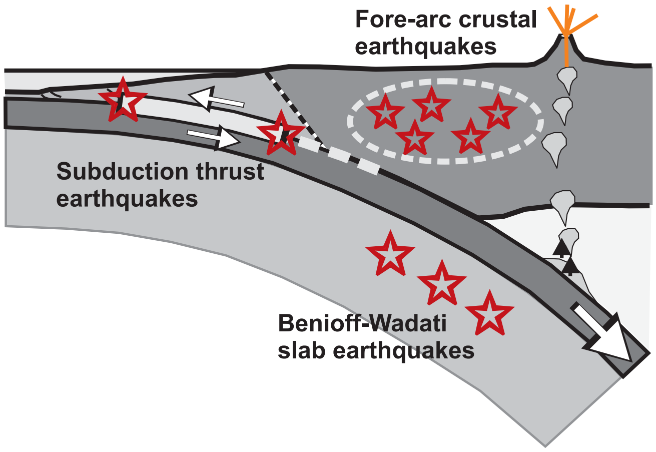

primarily from the statistics of the past earthquake record. However, the hazard from subduction thrust earthquakes in this region has been difficult to estimate from the past seismograph record. There are some written descriptions of large earthquakes in the 1800s in the news media but the first seismograph in the region was a low-sensitivity instrument established in Victoria in 1898. The first high sensitivity instruments in southwestern Canada and northwestern United States were installed in the 1950s to 1960s. The first routine digital recording on the west coast of Canada started in 1975 (e.g., Milne et al. 1978; Rogers and Horner 1991; Rogers 1992; Cassidy et al. 2003). The seismic network expanded in the mid 1980s to allow depth determination over most of the Vancouver Island and northwestern Washington region.

Even if good earthquake statistics were available, in this area the statistics of smaller earthquakes do not give a good estimate of the frequency of megathrust earthquakes. The occurrence rate of large and damaging but infrequent earthquakes in a region normally can be estimated reasonably well from the statistics of more frequent small events using the systematic recurrence relation between earthquake magnitude and frequency of occurrence for active fault zones (e.g., Gutenberg and Richter 1954). The average number of earthquakes in a particular source region decreases with increasing size in a predictable way up to the maximum magnitude. The maximum magnitude can be estimated from the size of the event that breaks the largest fault area in the region. The average occurrence of large earthquakes can thus be estimated even if there have been no such events in the historical record. The earthquake hazard, the probability that a particular magnitude of ground shaking will be exceeded in a specified period of time, is usually based mainly on this relation and used in building codes, such as the Canadian National Building Code (e.g., Adams and Atkinson 2003). This relationship holds well for most continental crustal earthquakes in the area and Wadati-Benioff earthquakes in the subducting plate (with exception of the area of the 1918 and 1946 earthquakes on central Vancouver Island that has had very few small events; Fig. 3). However, it does not hold for the Cascadia subduction thrust fault because very few earthquakes of any size have been detected on the Cascadia subduction thrust. The possible exceptions are two earthquake clusters off Oregon (Tréhu et al. 2008) and a M = 7.2 event in the Cape Mendocino region that may have been on the subduction thrust or a slightly shallower fault in the accretionary prism (Oppenheimer et al. 1993; Velasco et al. 1994; Wang and Rogers 1994).

In a global perspective, the lack of any subduction thrust earthquakes is unusual. Most of the world's great earthquakes ($M \geq 8$) have occurred on subduction zone thrust faults, and most subduction zones have experienced historical great earthquakes. The Cascadia subduction zone is an anomaly. However, the global subduction zones that have had the largest earthquakes ($M \sim 9$) Sumatra in 2004–2005, Alaska in 1964, Chile in 1960, and Kamchatka in 1952, also have had very long times between events and few small thrust earthquakes. For Cascadia, the written historical record is short, with only a little more than 200 years since the first European visits to the region by Captains Juan Perez in 1774 and James Cook in 1778 (although the coast native oral history of the effects of past great earthquakes and tsunamis has proven remarkably descriptive, as noted later in the text). This limited written history is in marked contrast to the detailed Japanese record of great subduction zone earthquakes and tsunami waves that extends back to the 7th century (e.g., Ando 1975). There are three possible explanations for the lack of historical Cascadia great earthquakes: (1) the Juan de Fuca plate is no longer converging and underthrusting North America; (2) underthrusting is continuing, but it is accommodated by smooth stable sliding, not punctuated by the stick-slip behaviour of earthquakes; (3) the thrust fault is completely locked with not enough motion to generate even small earthquakes and the last great event was before the written historical record. The first two options imply that the earthquake hazard estimates for the region based on historical seismicity are appropriate. The third option implies that there is a potential for very large and damaging earthquakes that was not been included in hazard estimates until recently.

Thirty years ago the first option of no convergence was much discussed, and Riddihough and Hyndman (1976) compiled a variety of evidence that there is ongoing convergence and underthrusting. Since then, the evidence has become conclusive. For example, folding and faulting are seen in seismic reflection images of sediments at the base of the continental slope, including Quaternary sequences <1 Ma old (e.g., Davis and Hyndman 1989). They continue to be scraped off the underthrusting oceanic crust by the bulldozer blade of the continental crust. Another dramatic evidence for active subduction was the volcanic eruption of Mt. St. Helens in 1980, one of the chain of active (although some historically quiescent) arc volcanoes from northern California to southern British Columbia. The north–south extent of the volcanoes matches the extent of the subducting Juan de Fuca plate (Fig. 4).

The debate over the second possibility, smooth aseismic underthrusting, continued until more recently. Again, the contrary evidence is now strong, especially from paleoseismicity, the traces of past great earthquakes preserved in the coastal and deep sea geological record, and from measurements of present elastic strain building up in the continent near the coast. The observed deformation corresponds to that expected for a locked thrust fault. These two types of evidence are discussed in the following sections. We are

Fig. 4. Juan de Fuca plate and Cascadia subduction zone. The Cascade arc volcanoes are limited to the extent of subduction.

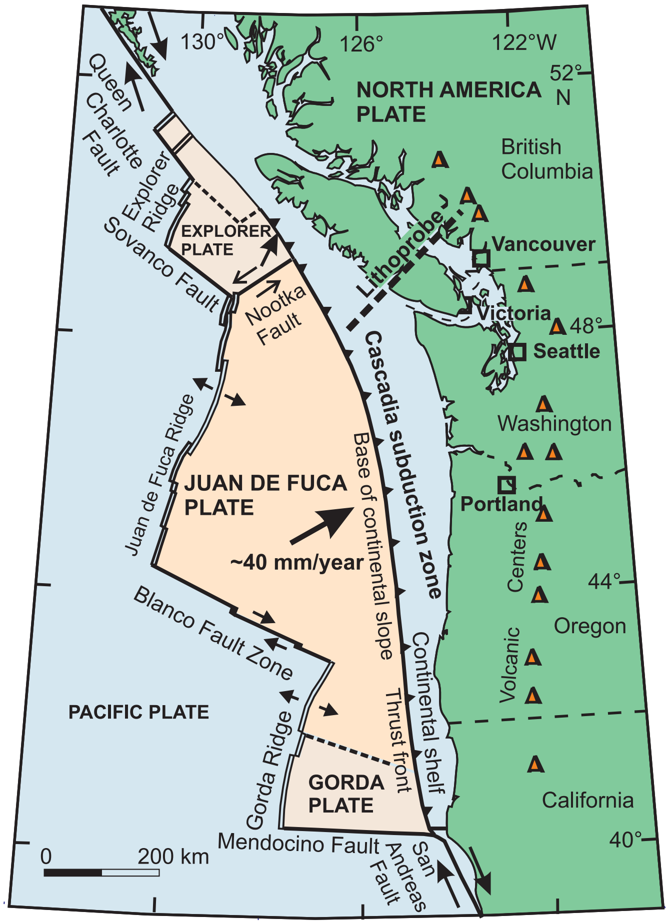

left with the third alternative that great earthquakes do occur, but the last one was more than 200 years ago, prior to the historical written record.

Oral record of 1700 great earthquake and the tsunami record in Japan

Support for the conclusion of a great earthquake before the written record is preserved in the oral tradition of a number of coastal native people in the region. They had a strong oral record, but only a small amount remains. There are clear accounts of an event not long before European contact and written records (e.g., Kroeber 1976). They describe a disastrous shaking and tsunami event on a winter night (e.g., Heaton and Snavely 1985; Clague 1995; Ludwin et al. 2005). For example, there is a description of a strong earthquake that occurred at night followed by a large tsunami that destroyed the village at the head of Pachena Bay on the west coast of Vancouver Island (Arima et al. 1991). In another account, the canoes came down in the trees. The occurrence on a winter night agrees with the time estimated from the tsunami that damaged the coast of Japan, January 25, 1700, as discussed as follows.

A precise determination of the date of the most recent great Cascadia great earthquake comes from the tsunami reported on the coasts of Japan. A tsunami in the year 1700 with wave heights of 2 to 3 m, not caused by a local Japanese earthquake, has been documented for five sites along the coast of Japan by Satake et al. (1996) and Atwater et al. (2005). These authors provided arguments for excluding sources other than Cascadia and show computer-generated wave models across the Pacific Ocean. Correcting for the tsunami travel time to Japan and the time zone difference, the source ~M9 great earthquake must have occurred along the North American coast on 26 January, 1700, at about 9 p.m.

Past great earthquakes in the geological record: coastal subsidence and deep sea turbidite sediments

We have information on the types of geological records that remain after great subduction earthquakes from historical great events elsewhere (e.g., Satake and Atwater 2007; Shennan and Hamilton 2006), especially the ~M9 earthquakes that occurred in Sumatra in 2004–2005, Alaska in 1964, and Chile in 1960. These records include evidence of coseismic vertical motions, especially down-dropped and buried coastal marshes and corals, and adjacent deep seafloor landslide turbidite deposits. There is also coastal evidence of sand sheet deposits associated with past great tsunamis. The case is now strong that Cascadia great events have occurred at intervals of several hundred to almost 1000 years according to paleoseismicity data from the coasts and adjacent deep seafloor of southern British Columbia, Washington, Oregon, and northernmost California.

Buried coastal marshes

In sheltered inlets and bays, marsh vegetation develops at a level near high tide. Excavations beneath the marshes have revealed buried peat layers at depths of up to 2 m consisting of vegetation that is identical to that of the present marsh surface (e.g., Fig. 5; e.g., Atwater 1987; Peterson and Darienzo 1991; Atwater 1992; Nelson et al. 1995; Atwater and Hemphill-Haley 1997; Clague and Bobrowsky 1994*a*, 1999; Benson et al. 1999). The data for the whole Cascadia margin have been recently summarized by Leonard et al. (2004, 2010) and Goldfinger et al. (2009). The 1700 event appears not to have extended to the north of Nootka Island off central Vancouver Island (coastal intersection of adjacent offshore Nootka transform fault; e.g., Benson et al. 1999). An example of a buried marsh is shown in Fig. 6. The peat layers are interpreted to be former intertidal marsh vegetation that was submerged by abrupt coastal subsidence at the time of past great earthquakes. Following each great earthquake, coastal mud accumulated on the drowned marsh, building the surface to mid-tide level and above, whereupon intertidal marsh vegetation became reestablished. Estimating the coseismic subsidence accurately requires paleoelevation estimates from marsh organisms just above the buried marsh tops, not just the depth of the buried marsh below the current marsh, because of ongoing sea-level rise and interseismic uplift (see Guilbault et al. (1996) for a detailed depth zoning study of a west coast of Vancouver Island marsh).

Many of the buried marsh surfaces are covered by sand layers (see Fig. 6; e.g., Clague and Bobrowsky 1994*b*; Clague et al. 2000; Peters et al. 2003), interpreted to be car-

Fig. 5. Schematic of changes in intertidal marsh following earthquake subsidence and subsequent sediment deposition (modified from Leonard et al. 2004 and Atwater 1987).

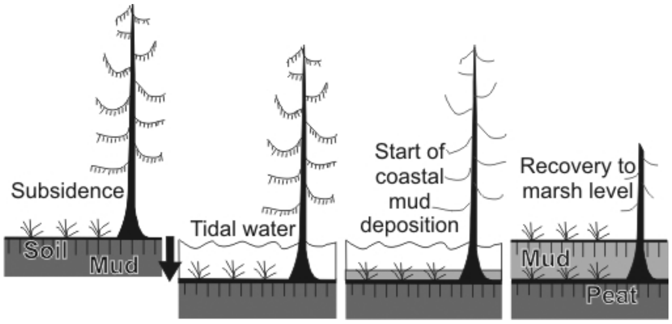

Fig. 6. Example of northern Cascadia buried 1700 marsh top and overlying tsunami sand (modified from Leonard et al. 2004).

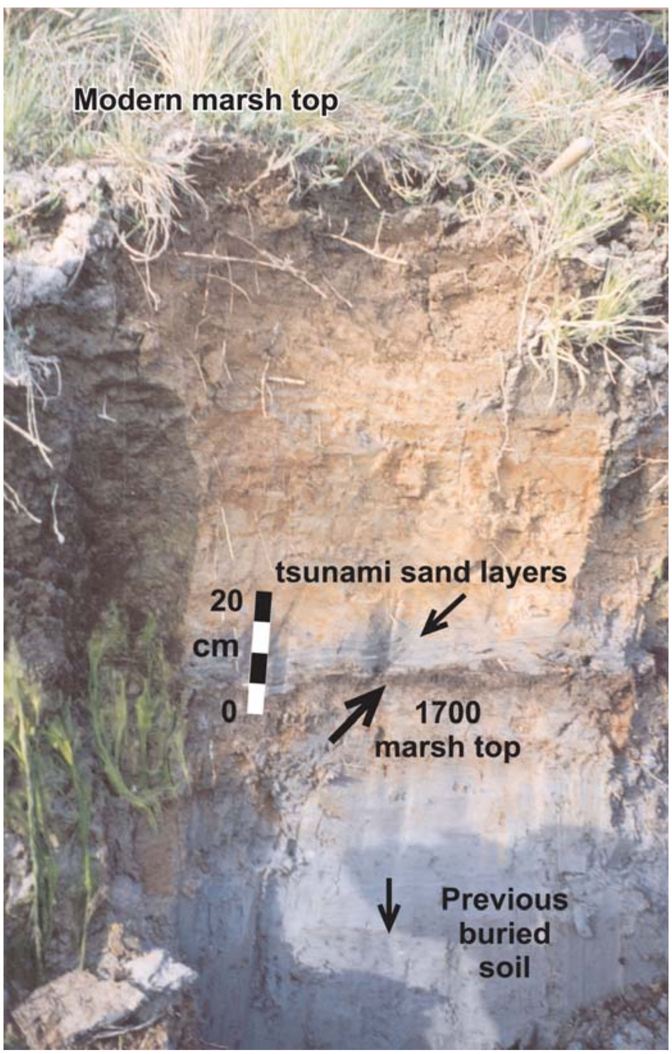

Fig. 7. Example of alternating turbidite (thick) and interseismic pelagic mud (thin) layers marking past great earthquakes (after Adams 1990). See Goldfinger et al. (2009) for recent detailed core studies.

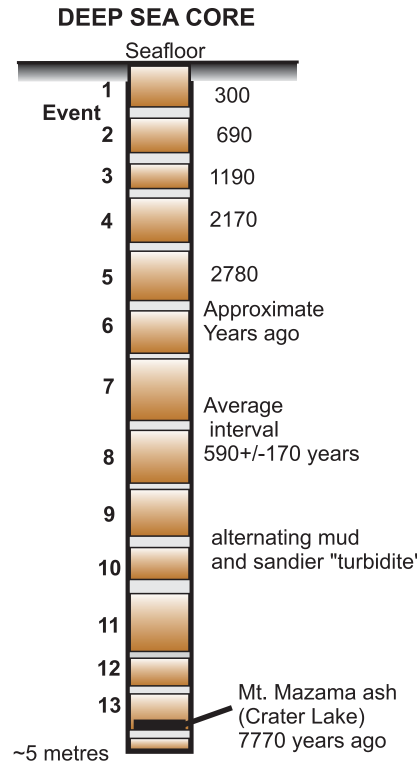

ried in by the great tsunamis that washed onto the subsided coastal region. Both theoretical modelling and effects preserved in the geological record on the coast indicate that the waves may have had heights commonly of about 6 m on the open coast and much higher to possibly 16 m in some confined inlets (e.g., Satake and Tanioka 1996; Priest et al. 2000; Geist 1999, 2005; Geist and Yoshioka 1996; Cherniawsky et al. 2007). The expected local runup is very sensitive to the details of the coastline and near-shore bathymetry and has been precisely modelled for only a few locations. The modelled wave heights decrease substantially in Georgia Strait and Puget Sound but are still significant. Radiocarbon dating of marshes and growth ring studies of drowned trees at sites from northern California to southern British Columbia both show the last Cascadia great event to have occurred a little over 300 years ago in 1700 (e.g., Atwater et al. 1995; Jacoby 1995; and summary reviews and references by Leonard et al. 2004, 2010, and Goldfinger et al. 2009).

Earthquake triggered deep sea turbidites

Other evidence for past great earthquakes comes from repeated sediment deposits on the floor of the Cascadia deep sea basin at the base of the continental slope. Core samples by Oregon State University (Griggs and Kulm 1970) showed fine-grained mud layers alternating with sandier layers (Fig. 7); such repeated sequences are usually denoted as turbidites. An important recognition by Adams (1990) was that the sandier layers have been formed by submarine landslides triggered by great Cascadia earthquakes. The intervening mud layers are formed by the slow continuous rain of finer sediment between the turbidite events. The turbidite layers in most cores have been concluded to be simultaneous along all or most the Cascadia 1000 km coast, and therefore probably triggered by M9 great earthquakes that ruptured most of the margin. Subsequent detailed coring studies by Goldfinger and others (Goldfinger et al. 2003, 2009) have confirmed this conclusion and better defined the great earthquake timing. The timing of the individual earthquakes is still difficult to determine precisely because of the low accuracy of radiocarbon dates for the past few 1000 years, but an important marker for the average rate is the volcanic ash in the cores from the huge eruption of Mt. Mazama in Oregon (Crater Lake) 7700 years ago. The inferred chronology is very similar to that obtained from the coastal marshes. The most recent major turbidite event in the cores was about 300 years ago. The intervals for the last 13 events range mostly from about 300 to 900 years. The very long intervals between Cascadia events compared with most subduction zones means that there is large elastic strain buildup and, thus, very large earthquake slip and large magnitude.

For events that produced clear turbidites along the full or near-full length of the margin in the last 10 000 years, the average recurrence interval is about 500 years with variability of a few hundred years (Goldfinger et al. 2003, 2009; Leonard et al. 2010). There is evidence for additional events in the southernmost part of the Cascadia zone (Nelson et al. 2006; Goldfinger et al. 2003, 2009), which means segmentation of that region. There is little evidence for additional events in the northern part off Washington and southern Vancouver Island. The northern portion of Juan de Fuca plate subduction, therefore, may rupture mainly in whole margin events. There also is no evidence yet for great earthquakes on the Explorer plate segment of the subduction zone to the north of the Nootka transform fault, although evidence for plate convergence there is clear in (*i*) deformation of offshore Quaternary sediments, (*ii*) contemporary geodetic deformation, and (*iii*) ongoing episodic tremor and slip (ETS) activity (see later in the text).

One of the most promising recent discoveries that will likely refine the estimates of the times of past great subduction earthquakes in northern Cascadia is the recognition that these events have left signatures in Saanich Inlet and Effingham Inlet, and perhaps other anoxic fiords on Vancouver Island (Blais-Stevens et al. 2009; Dallimore et al. 2009). The lack of bioturbation in the sediments at the bottom of these anoxic inlets means that annual varve sediment layering is preserved. Thus, turbidity deposits from underwater landslides caused by the lengthy strong shaking of subduction earthquakes can be dated by their position in this laminated sedimentary sequence.

The great earthquake cycle and locked fault strain build up

Like all earthquakes, great subduction zone events are complex when considered in detail. However, the basic process is simple and may be represented by the elastic rebound model first developed for the San Andreas Fault (Reid 1910). Ongoing convergence and underthrusting of the oceanic plate results in elastic bending and buckling of the continental crust and the accumulation of elastic stress in the vicinity of the locked fault. After some time, the stress exceeds the sliding strength of the fault, and there is abrupt slip. The stored elastic energy radiates as seismic waves. After a short period of after-slip and viscous readjustment (e.g., Hu et al. 2004), the fault relocks and the cycle resumes (Fig. 8). For the Cascadia subduction zone,

Fig. 8. Simplified model of great earthquake elastic strain buildup and release compared with uplift from levelling data. Current shortening and uplift of coastal region are detected by GPS and other geodetic techniques. Coseismic collapse of the uplifted area buries coastal marshes and generates great tsunamis.

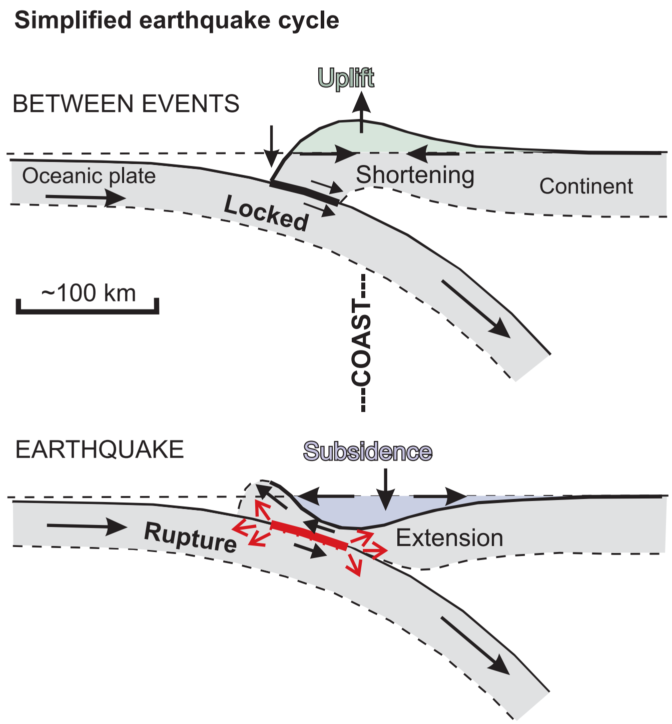

the rate of convergence between the Juan de Fuca plate and North American plate is about 40 mm/year (40 km/Ma; Riddihough 1984). This convergence represents a shortening between events and an average rupture displacement of about 20 m if the event interval is 500 years and there is no aseismic slip. Rupture slips this large are thus expected in a Cascadia great earthquake.

The first clear indication of horizontal strain build up on the locked Cascadia subduction fault was by Savage et al. (1991) using laser ranging. Dragert and Hyndman (1995) showed the expected pattern of horizontal shortening using initial precision global positioning system (GPS) data. From repeated levelling data, Reilinger and Adams (1982) pointed out that the coast was tilting landward, although how this was to be interpreted was not clear. It was later recognized that this tilting was as expected for a subduction thrust that is locked offshore (Savage et al. 1991; Hyndman and Wang 1993). It was subsequently shown that the Cascadia subduction thrust was probably locked along most if not all of the margin, and the downdip width of the locked zone was defined using a series of high-precision repeated lines and long-term tide gauges, mainly by US Geodetic Survey, perpendicular to the coast (e.g., Hyndman and Wang 1995; Mitchell et al. 1994). More recently, widespread precision GPS data, including inversions for the effective backslip on the fault, have defined the locked zone and uncertainties more precisely (e.g., Mazzotti et al. 2003; Wang et al. 2003; Yoshioka et al. 2005; McCaffrey et al. 2007; Goldfinger et al. 2009). Across Vancouver Island, repeated precision levelling and gravity have also resolved the pattern of vertical deformation. These data, and GPS and other vertical data, suggest that this profile is special for the Cascadia margin, having only a small amount of ongoing tilting upward toward the coast (e.g., Wolynec 2000), perhaps owing to the effect of long-term tectonic or postglacial rebound processes.

Elastic deformation of the subduction earthquake cycle is mainly limited to a zone several 100 km wide, close to the plate boundaries (e.g., for northern Cascadia, Hyndman and Wang 1995; Flück et al. 1997; Mazzotti et al. 2003). The deformation through the earthquake cycle includes a viscous component that gives a time dependence to the deformation pattern and rate (e.g., Wang et al. 2003). However, after a few tens of years, to a first approximation the response is elastic and at a nearly steady rate between earthquakes. In the simple subduction earthquake model, ongoing convergence drags down the seaward nose of the continent and causes an upward flexural bulge farther landward (Fig. 8). There also is a region of crustal shortening (Fig. 8). At the time of the earthquake, the edge of the continent springs back seaward and the bulge collapses downward. The abrupt coseismic uplift of the outer continental shelf and slope and subsidence near the coast are mainly responsible for the great tsunamis. Shaking-triggered subsea landslides may be additional tsunami sources. The collapse of the flexural bulge causes the sudden coastal subsidence recorded in buried intertidal marshes.

Subduction zone structure and definition of the megathrust

Accurate definition of the subduction thrust plane is required for models of the deformation associated with the great earthquake cycle, for thermal models that estimate temperatures on the subduction thrust and, therefore, the downdip limit of seismic behaviour, and for a number of other earthquake-related applications. The profile uncertainty also has consequences for the shaking estimated from great thrust events. The definition of the downgoing plate was one of the primary objectives of the initial Lithoprobe Vancouver Island transect. An excellent summary of the dip profile data along the whole Cascadia margin has been provided by McCrory et al. (2006). However, even with the importance of this definition and the much increased data now available, we still have debates on which geophysical signatures represent the subducting Juan de Fuca plate and the subduction thrust fault along the Cascadia margin, especially beneath Vancouver Island, even though we have the most data in that region. Three different depth profiles have been suggested, that may be designated shallow, mid, and deep. Fortunately, for the Lithoprobe area the uncertainty in depth of the thrust is mainly beneath Vancouver Island; there is little uncertainty beneath the outer continental shelf where most rupture displacement is inferred to occur.

The subduction zone structure and constraints on the megathrust fault come from a number of sources:

(1) Multichannel seismic reflection and wide-angle refraction surveys both offshore and onshore of Vancouver Island provide important constraints that have defined the subduction zone structure and current tectonic regime (e.g., review by Hyndman 1995*b*); the critical uncertainty is whether the E-zone of landward-dipping reflectivity (Fig. 9) is associated with or is above the subducting oceanic plate.

(2) The second constraint on the subduction thrust location and structure come from Benioff-Wadati earthquakes in the downgoing oceanic plate; an important uncertainty is where these earthquakes occur in the crust and where they occur in the uppermost mantle. The uppermost events are interpreted to occur in the upper oceanic crust (Cassidy and Waldhauser 2003; Wang and Rogers 1994; Preston et al. 2003).

(3) Seismic tomography has defined the top of the high-velocity upper mantle of the subducting plate in the Georgia Strait – Puget Sound region (Ramachandran et al. 2005; Preston et al. 2003).

(4) Receiver function data interpretations of the converted waves from distant earthquakes at broad-band seismic stations in the coastal region define a low-velocity zone that may be associated with the reflective E-zone. This zone may be a shear zone located above the thrust (Cassidy and Ellis 1993; Cassidy and Waldhauser 2003) or the low-velocity downgoing oceanic crust (Nicholson et al. 2005; Audet et al. 2008, 2009). There is a deeper low-velocity zone associated with the original F reflector (Clowes et al. 1987*a*) that also has been interpreted as the downgoing oceanic crust (Cassidy and Ellis 1993; Cassidy and Waldhauser 2003).

Offshore Vancouver Island, the top of the oceanic crust is well defined in multichannel seismic profiles, and the subduction thrust has been concluded to be close to the top of the downgoing oceanic crust based on most of the frontal thrust faults extending down to nearly that depth. This reflector can be followed to beneath the mid continental slope. However, there is still some uncertainty in this interpretation since at other subduction zones, substantial sediments are sometimes subducted so the detachment is above the top of the oceanic crust, and sometimes there may be erosion of the overlying fore-arc crust, such that the thrust cuts upward as it moves landward (e.g., von Huene and Scholl 1991). Further landward beneath the inner shelf and especially beneath Vancouver Island where there is Lithoprobe land vibroseis reflection data, there have been several interpretations. Beneath Vancouver Island, there is a strong band of landward-dipping reflectors, the "E-layer," that was first interpreted using just Lithoprobe land data to be associated with the top of the plate (Yorath et al. 1985). Clowes et al. (1987*a*) proposed that the top of the plate was at the base of the E-layer (Fig. 9). With the addition of adjacent marine seismic reflection data, the top of the oceanic plate was subsequently associated with the deeper F reflectors (e.g., Hyndman et al. 1990). Subsequent receiver function data indicated a low-velocity zone at the depth of the E-layer (Cassidy and Ellis 1993), and magnetotelluric data was interpreted to have resulted from a high-porosity layer above the subducting slab (Kurtz et al. 1986; Hyndman 1988). Cassidy and Ellis (1993) noted that there was a deeper less-pronounced low-velocity zone below the E-layer that was in better agreement with the Benioff-Wadati earthquake data and with the F-layer; they concluded that the F-layer is the top of the oceanic crust. Subsequent studies have resulted in

Fig. 9. (*a*) Multichannel seismic cross-section across Vancouver Island in area of Lithoprobe corridor (after Clowes et al. 1987*a*). (*b*) Composite seismic section in Vancouver Island region from offshore to mainland (after Calvert 2004), illustrating the E-zone reflection band, interpreted to be above the downgoing Juan de Fuca plate (see text for various interpretations). JdF, Juan de Fuca plate; LRF, Leech River Fault; M?, Moho?; Serp.?, possibly serpentinized.

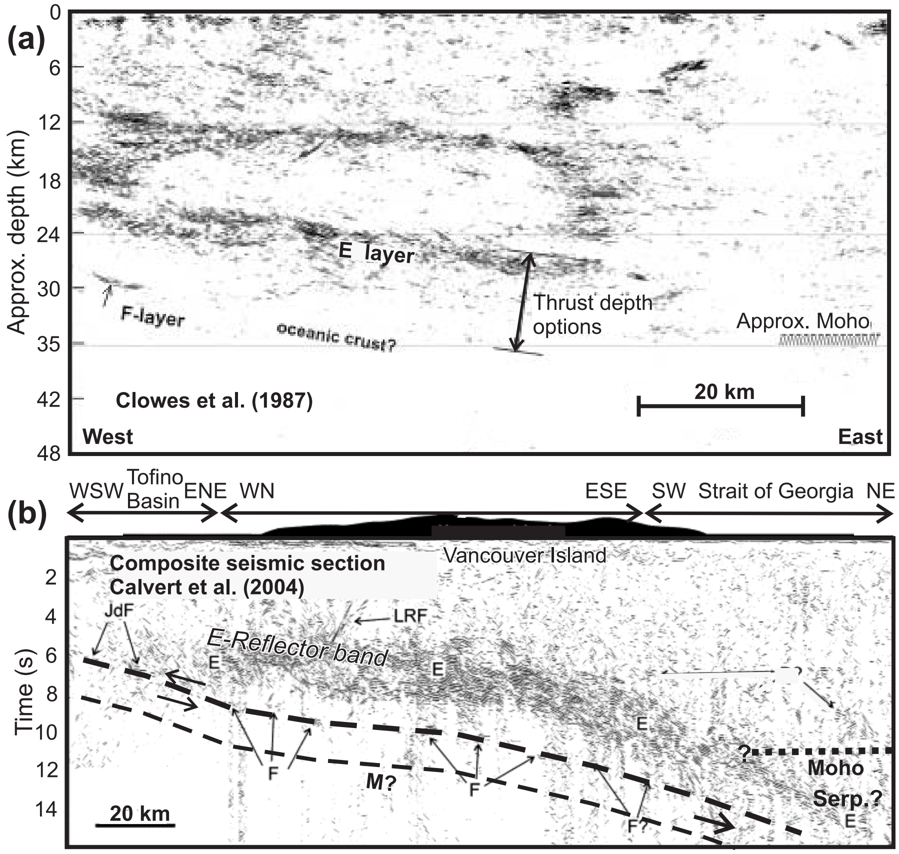

a number of options for the depth of the megathrust and the depth of the underthrusting oceanic plate.

The deep Benioff-Wadati seismicity beneath southern Vancouver Island and adjacent areas is interpreted to be in two zones, one in the subducting upper oceanic crust and one in the uppermost mantle (Cassidy and Waldhauser 2003; Preston et al. 2003). The seismicity defines a plate depth that is consistent with the oceanic Moho interpreted as the deeper F reflectors. This seismicity is centered more than 10 km deeper than the E-layer under Vancouver Island.

An especially strong constraint to the position of the oceanic plate, but not necessarily the thrust detachment, comes from the large velocity contrast at the subducting oceanic Moho in seismic tomography studies. The tomography included joint inversion for improved earthquake hypocentres. Both compressional and shear-wave seismic tomography results are consistent with the depth to the top of the subducting oceanic mantle (oceanic Moho) from the seismicity interpretation, 5–10 km below the F-layer (Ramachandran et al. 2005, 2006; Preston et al. 2003).

More recently the low velocity zone associated with the E-layer, defined by very detailed receiver function data across the margin, has been interpreted to represent the low shear-wave velocity subducting oceanic crust (Nicholson et al. 2005; Audet et al. 2008, 2009), so the depth interpretation to the subducting plate remains uncertain. They interpreted the low velocity and high Poisson's ratio in the E-layer to represent high pore pressure in the oceanic crust associated with progressive dehydration processes downdip. This interpretation places the subduction thrust at a shallower depth than either of the two previous estimates.

Another alternative model is a complex deformation zone above the subducting plate and associated with the E-zone that accommodates the subduction thrusting. Green et al. (1986), Calvert et al. (2003), Calvert (1996), and Calvert and Clowes (1990), argued that the main zone of thrust deformation is above the subducting oceanic crust (Fig. 9). In this interpretation, the inter-plate boundary may be up to 16 km thick and may comprise two megathrust shear zones that bound a >5 km thick, ~110 km wide region of imbricated crustal rocks (Calvert 1996, 2004). This model is supported by the ETS tremor that may represent thrust shearing, being concentrated at the depth of the E-layer (Kao et al. 2009). Such a model is attractive since it accommodates the strong E-layer reflection band with low velocity from receiver function as a detachment zone well above the top of the underthrusting oceanic crust. However, it has the difficulty of requiring that the current structure be a geologically short-term transient, since there is a space problem with long-term imbrication. If it persists, this imbrication should cause very large deformations at the surface that are not evident. In this interpretation, a significant part of the lower fore-arc crust may be carried rapidly downward to some unknown depth.

We recognize that the thrust dip plane under Vancouver Island is not yet conclusively resolved. Fortunately, the uncertainty is not large beneath the continental shelf where megathrust events are concluded to occur. From recent detailed modelling tests, the effect of the range of thrust dip possibilities on the landward extent of the locked zone from thermal and geodetic constraints, and on seismic hazard, is not large (K. Wang and S. Mazzotti, personal communication, 2009).

Processes that control the updip and downdip rupture limit

Only a portion of the thrust fault ruptures in great earthquakes. Definition of the rupture area is critical both for the size of the events and for magnitude of the shaking inland. The extent of the locked seismic zone that is interpreted to rupture (actually the locked plus transition zones as defined later in the text) is limited both updip and downdip. Some subduction zones exhibit thrust earthquakes of various sizes within these limits. However, for Cascadia and other margins having M9 earthquakes, the subduction thrust appears to usually rupture the full downdip seismogenic extent, with very few smaller thrust events. The landward downdip limit of rupture is important for seismic hazard since it determines the source's closest approach to the major population centres located 100–200 km inland of the outer coast. The seaward updip limit is important for tsunami generation. The total seismogenic width perpendicular to the margin has an important influence on the maximum size of great earthquakes.

Seaward updip seismic limit

The seismic zone is bounded seaward by a region that does not generate earthquakes, and there must be a transition zone of some width between the fully locked and updip free slip zone. There are no good direct constraints for the seaward limit of rupture in past great Cascadia earthquakes, only very broad constraints to near the seaward limit of the subduction thrust from the size of the 1700 tsunami (e.g., Priest et al. 2000). However, there are suggested physical limits to elastic strain buildup and rupture that appear to explain observations from other subduction zones. Free slip in the updip aseismic zone may be a consequence of the stable sliding clay minerals that are common in the region of subduction zone faults. At a depth of $\sim$10 km, the sediments are no longer unconsolidated muds and sands, but have been compressed and lithified to sedimentary rock that may have sufficient strength to sustain elastic strain buildup. With increasing temperature, clays become compacted and dehydrated, and they transform to stronger minerals in complex processes, such as to exhibit seismic behaviour (see discussion by Underwood 2007). The fault may become seismogenic where the temperature reaches 100–150 °C (see discussion by Hyndman and Wang 1993). On other subduction zones, Harris and Wang (2007) showed how the updip limit varied in position with varying thermal regimes in the incoming plate, but was still at $\sim$150 °C. At the basal detachment of most of the frontal thrusts of Cascadia, the temperature is over 200 °C. Therefore, if this 150 °C temperature limit is correct, the seaward limit of the Cascadia locked zone is beneath the base of the continental slope in the region of the accretionary sedimentary prism complex frontal thrusts.

Landward downdip seismic limit

Many factors have been suggested for the controls of the downdip limit of the locked seismogenic zone (e.g., discussions by Tichelaar and Ruff 1993; Hyndman 2007), but two appear to dominate, (*i*) for hot subduction zones (such as Cascadia), there is a maximum temperature limit for seismic rupture behaviour (e,g., Hyndman and Wang 1993); and (*ii*) for most of the more common cool continental subduction zones, aseismic fore-arc mantle serpentinite appears to provide the downdip limit (e.g., Hyndman et al. 1995; Peacock and Hyndman 1999; Hyndman and Peacock 2003). At some depth, a temperature is reached on the thrust fault where the rocks behave plastically. More precisely, the critical depth is where the fault zone no longer exhibits frictional instability (Scholtz 1990). Laboratory measurements on continental crustal rocks indicate that the critical temperature marking the transition to stablesliding is about 350 °C (e.g., references listed by Hyndman and Wang 1993). Great earthquakes that are initiated where the temperature is <350 °C may rupture downdip with decreasing offset to where the temperature reaches about 450 °C. The 350 to 450 °C region, thus, corresponds approximately to the transition zone used to model the geodetic data. This temperature control agrees well with other constraints for landward limits to great earthquake rupture on the Nankai margin of southwest Japan and several other hot subduction zones (Hyndman et al. 1995; Oleskevich et al. 1999; Currie et al. 2002; Hippchen and Hyndman 2008). Thermal modelling applied to a number of cool subduction zones found that the thermal limit was deeper than the fore-arc Moho, and serpentinized fore-arc mantle is inferred to provide the downdip rupture limit in most cases. There are a few subduction zones where the downdip limit has been concluded to be deeper than either of these limits.

Because the subducting Juan de Fuca plate is young and there are thick insulating sediments on the incoming oceanic crust, the temperatures on the Cascadia subduction thrust are very high. The result is a thermal seismogenic landward limit that is especially shallow.

Cascadia downdip rupture limit

The downdip landward limit of the Cascadia rupture zone can be estimated from five constraints:

(1) The current locked zone on the thrust based on comparison of geodetic data that constrain the pattern of current interseismic deformation and the predictions of locked fault elastic dislocation models (e.g., Savage 1983).

(2) The downdip limit of past great earthquake ruptures based on the subsidence recorded in coastal marshes compared with predictions of elastic dislocation models.

(3) The thermal limit for seismic behaviour of 350–450 °C based on laboratory data, and the downdip variation in

Fig. 10. Pattern of vertical motion from repeated levelling across northern Cascadia and southwest Japan compared with elastic dislocation models for the megathrust locked and transition zone, showing the effect of different landward extents of locked and transition zones. These kinds of data provided the first definition of the width of the locked zone along this margin. subsid., subsidence.

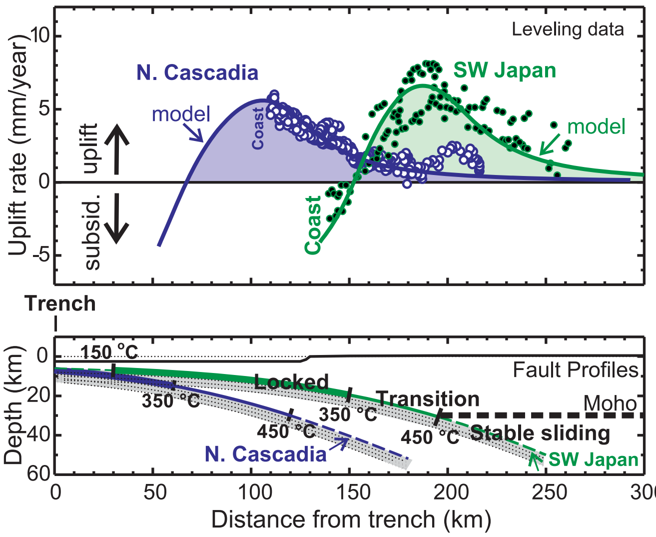

temperatures on the Cascadia thrust plane from numerical thermal models.

(4) The change in multichannel reflection character at the downdip transition from brittle seismic behaviour to deeper aseismic slip, from a thin boundary to a thick shear zone (including the E-layer).

(5) The updip limit of ETS slow slip and tremor that may define the downdip earthquake rupture limit.

Geodetic constraints to downdip limit of locked zone

The extent of the locked zone on the thrust fault that may approximate the rupture zone can be determined from the pattern of interseismic crustal deformation (e.g., Fig. 8). If the locked zone is narrow, extending only a short distance downdip, the zone of elastic deformation is narrow. If the locked zone is wide, the deformation zone will extend a long distance inland (e.g., Wang et al. 1994). Comparison of the deformation from geodetic surveys with the predictions of models for a locked thrust fault shows, firstly, that the subduction thrust fault is probably locked along the whole coast from southern British Columbia to northern California, with very little if any aseismic slip. Secondly, the variations in downdip width of the locked zone along the coast have been mapped (Hyndman and Wang 1995; Miller et al. 2001; Murray and Lisowski 2000; Svarc et al. 2002; Mazzotti et al. 2003; Wang et al. 2003; Yoshioka et al. 2005; McCaffrey et al. 2007; Goldfinger et al. 2009). Figure 10 also illustrates the effect of locked zone width through a comparison of the vertical deformation over the narrow locked zone of northern Cascadia at Vancouver Island and the wider locked zone of southwest Japan.

The rates of deformation are very slow and very precise measurements are required, able to resolve deformation rates of a few millimetres/year. Five types of geodetic data have defined the pattern of current deformation across the Cascadia margin. They include (1) continuously recording and repeated campaign GPS station networks, (2) repeated survey levelling lines, (3) long-term tide gauge records, (4) repeated gravity surveys. All three types of measurements of vertical motion (levelling, tide gauges, and gravity) give similar results although there are still large uncertainties (e.g., Wolynec 2000 for Vancouver Island). For the Cascadia margin, there is present uplift at rates that vary along the coast from 1 to 4 mm/year. The uplift rate decreases to near zero at 100 km inland from the point of maximum uplift. The value for the southwest coast of Vancouver Island is unusually small for the Cascadia margin (~1 mm/year), which has not yet been adequately explained, although it is ~3 mm/year as expected from elastic dislocation models for the coast of the Olympic Peninsula just to the south.

Fig. 11. Three examples of many continuous and repeated GPS measurements of coastal shortening associated with locked megathrust. See Mazzotti et al. (2003) for a summary of such measurements in the southern Vancouver Island area.

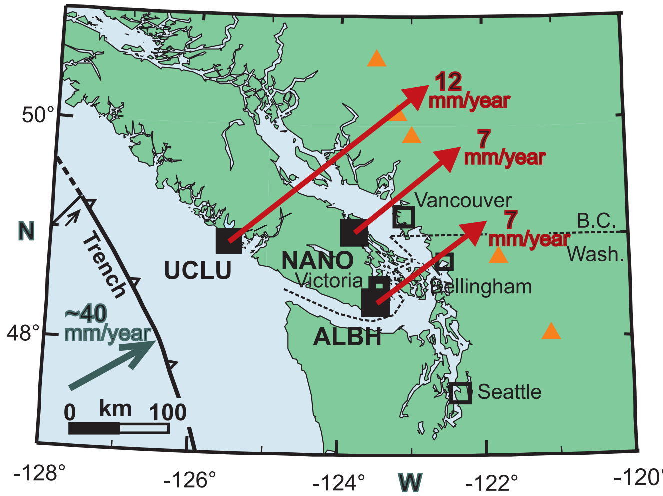

Horizontal deformation across the coastal region was first found from repeated distance measurements using laser ranging between mountain tops, initially shown for the Seattle – Olympic Peninsula region (e.g., Savage et al. 1991). In more recent years, the satellite GPS has permitted horizontal and vertical level measurements over distances of hundreds of kilometres with sufficient accuracy to detect earthquake-related strain build-up. The horizontal deformation is much easier and more accurate to measure than the vertical, and the horizontal now provides the most precise constraints, although fore-arc deformation adds some complexity. Dragert and Hyndman (1995) reported a rate of shortening of about 7 mm/year between Victoria on the coast and Penticton 300 km inland, which is nearly fixed relative to stable North America. The uncertainty is only about 1 mm/year over this distance. Numerous subsequent measurements have shown about 10 mm/year across the 100 km wide coastal zone rate (e.g., Mazzotti et al. 2003), about 25% of the 40 mm/year total plate convergence (e.g., Wilson 1993). Example sites are shown in Fig. 11; there now are more than 50 Cascadia continuous and many more repeat campaign GPS sites that define the ongoing deformation. Most of the remainder of the plate convergence is taken up as

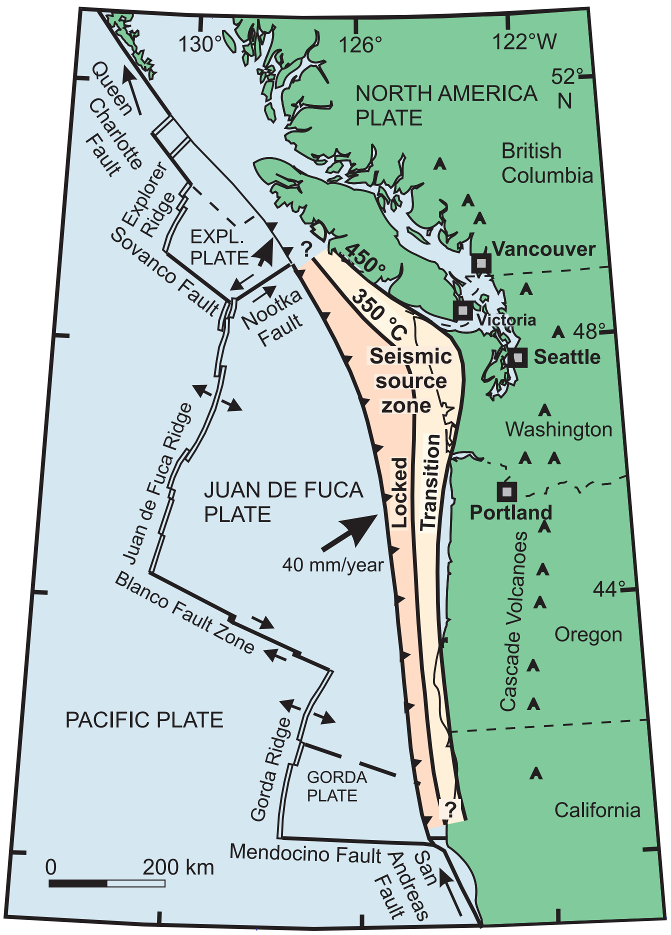

Fig. 12. The locked, transition and episodic tremor and slip (ETS) zones on the Cascadia subduction thrust based on geodetic (GPS and repeat levelling) and thermal constraints (modified from Hyndman and Wang 1995). See text for similar recent inversion models. EXPL., Explorer.

shortening farther seaward across the continental shelf. The horizontal rate measured on Vancouver Island, if continued, represents 10 km/Ma; the vertical rates represent 1–4 km/Ma This would produce very high coastal mountains in a short time, so the measured deformations must be short-term elastic transients that will be released in the rebound accompanying the next great earthquake.

The downdip extent of the locked zone has been estimated by comparing the geodetic data with mathematical models of the elastic deformation (e.g., Dragert et al. 1994; Hyndman and Wang 1995; Wang et al. 2003; Yoshioka et al. 2005; McCaffrey et al. 2007; Goldfinger et al. 2009). The models include a transition zone on the fault, between the fully locked and downdip fully free slip portions, since an abrupt transition is physically unrealistic. The rupture displacement of great earthquakes is assumed to decrease to zero at the downdip limit of this transition zone. The effect of various versions of this transition zone has been examined by Wang et al. (2003). Interseismic transient deformation also may be important (e.g., Hu et al. 2004), although Cascadia is approximately half way through the interseismic period so non-elastic transients are probably less important. Block motions of the fore arc have added complexity to the modelling of the deformation associated with the locked subduction thrust fault. The map of Fig. 12 shows one simple summary of the locked and transition zone based on geodetic data for the whole Cascadia margin by Hyndman and Wang (1995). Other similar but more detailed models have been obtained by McCaffrey and Goldfinger (1995), McCaffrey et al. (2000, 2007), Yoshioka et al. (2005), and Goldfinger et al. (2009). There are clear variations along the Cascadia margin in the pattern of uplift and shortening. The inferred widths of the locked and transition zones are widest off the Olympic Peninsula of northern Washington where the plate dip is shallow and narrowest off central Oregon (Fig. 12). A cross-section across the Vancouver Island continental margin also illustrates the positions of the locked transition and free slip zones (Fig. 13).

The thermal downdip limit for seismic behaviour

Numerical thermal modelling using the finite element routines of K. Wang has been carried out for a series of profiles across the Cascadia margin to obtain the temperatures on the subduction thrust fault (Hyndman and Wang 1993, 1995; Oleskevich et al. 1999; Currie et al. 2004; K. Wang, personal communication, 2009). Measurements of the heat flux from the earth, both on land and the seafloor, provide a model constraint (Lewis, et al. 1988; Fig. 13). An important uncertainty in the thermal models is the importance of hydrothermal heat transfer in cooling the subducting oceanic crust (Kummer and Spinelli 2009). The positions of the 350 and 450 °C temperatures from the conductive model are in good agreement with the downdip limits of the locked and transition zones inferred from the deformation data discussed earlier in the text. Figure 13 shows that the inferred seismogenic zone lies beneath the prism of sediments scraped off the incoming oceanic crust. The temperatures on the Cascadia thrust plane are unusually high because the young incoming oceanic plate is hot and because there is a thick insulating sediment cover. As a result, a temperature of about 225 °C is reached at the top of the oceanic crust at the base of the continental slope. The high temperatures on the thrust plane mean that the 350 and 450 °C temperature limits for the inferred full rupture and transition zone are reached at an unusually short distance landward on the fault, under the edge of the continental shelf.

The landward limit from coseismic subsidence recorded in coastal marshes

Subsided and buried coastal marshes owing to coseismic subsidence of great earthquakes were discussed earlier in the text. Important support for the conclusions of the geophysical elastic dislocation modelling is provided by a comparison of predicted coastal great earthquake subsidence with that inferred from the studies of buried coastal marshes. The present coastal uplift rate of 1 to 4 mm/year, accumulated over an interseismic period of 500 years, gives an expected earthquake subsidence range of 0.5 to 2 m. The marsh subsidences associated with great earthquakes, estimated from the past and present faunal-constrained intertidal water depths just above and below the marsh tops, give similar earthquake subsidences (Fig. 14 after Leonard et al. 2010). Similar subsidences are also estimated from the most

Fig. 13. Compilation of heat flow data across the northern Cascadia margin at Lithoprobe corridor and corresponding numerical thermal model. The thermal limits to the locked (350 °C), transition (450 °C), and episodic tremor and slip (ETS) zones are shown. Accr. Seds., accreted sediments; BSR, bottom-simulating reflector; ODP, Ocean Drilling Program.

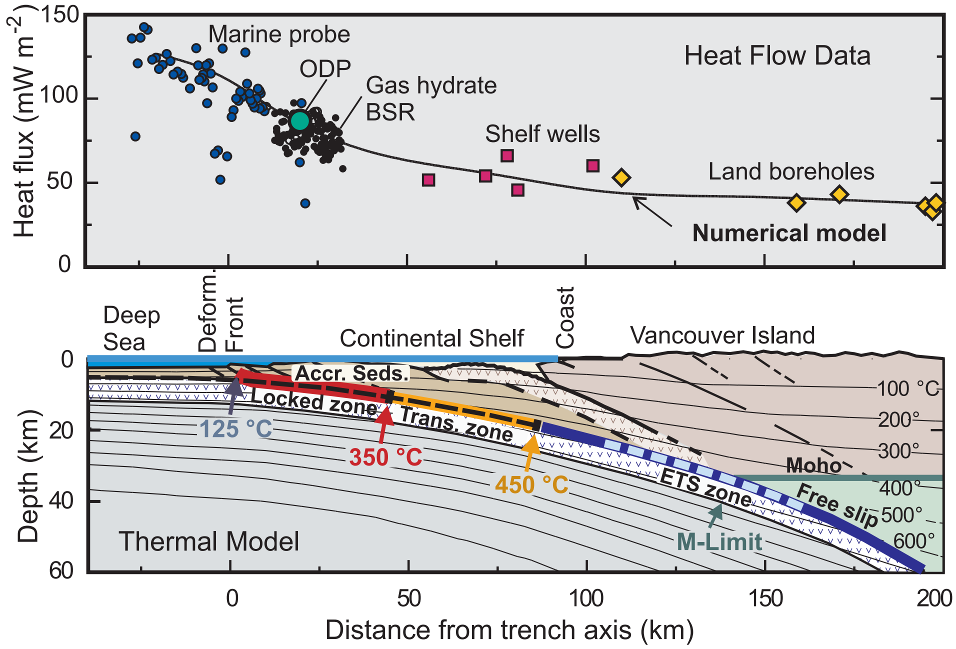

recent event burial depths, after allowing for eustatic sea-level rise, postglacial rebound and the interseismic earthquake cycle uplift, since the event. However, the accuracy from the latter approach is low. Variations along the coast are also in general agreement. For example, regionally, there is the smallest present uplift rate and shallowest marsh burial depth for the coast of central Oregon. However, there are differences in detail that remind us that we have simplified the complex earthquake process. Southern Vancouver Island is an anomaly with small interseismic uplift and small coseismic subsidence, as noted earlier in the text. Although the resolution is low, the marsh subsidences provide a strong constraint that the past great earthquake ruptures were well offshore, not extending beneath the coast, except for a small area of southermost Cascadia.

Change in multichannel reflection character at the downdip seismogenic limit

It has been concluded by Nedimovic et al. (2003) that there is a change in the seismic reflection character from a thin sharp reflector, where the subduction thrust is inferred to be seismic, to a broad reflection band at greater depth, where there is aseismic slip. They pointed out that deep seismic reflection images from Alaska, Chile, and southwest Japan show a similar broad reflection band above the subduction thrust in the region of stable sliding and thin thrust reflections further seaward, suggesting that reflection imaging may be a globally important predictive tool for determining the maximum expected rupture area in megathrust earthquakes.

For Cascadia, this interpretation is applicable only if the megathrust fault motion is associated with the E-zone rather than at the top of the downgoing oceanic plate, if the latter is deeper (see earlier discussion; Fig. 9). Combining the deep multichannel reflection images from surveys offshore of Vancouver Island, marine surveys in Georgia Strait – Puget Sound, and Lithoprobe land Vibroseis land surveys on Vancouver Island permitted mapping variations in the reflection nature of the interplate interface from the deep sea deformation front to where the megathrust interface reaches the fore-arc mantle corner. Despite considerable variation in the reflection character of the subduction thrust on the seismic lines, there is a consistent downdip change from a thin (<2 km) reflection zone offshore to a broad reflection band (E-layer) some 5–7 km thick, near or just seaward of the west coast of Vancouver Island (see seaward end of Fig. 9). This limit agrees very well with that from both geodetic data and thermal constraints.

Temperature estimates on the megathrust (see earlier in the text) and fluid-filled porosity estimates within the E-reflection zone led Nedimovic et al. (2003) to propose that ductile banding is the prevailing type of deformation in the E-layer shear zone. Laboratory and field studies of rocks from now-exposed deep faults and shear zones show that, at depths of 10–15 km or more and temperatures above about 350 °C, ductile processes begin to dominate and mylonites are usually formed. The temperature at the base of the E-reflection band beneath the east coast of Vancouver Island is about 400 °C, increasing to about 500 °C further landward. Mylonite zones from exhumed ductile shear zones are often as wide as the E-reflection band and are inferred to be very reflective. However, the E-reflection band must contain significant fluid-filled porosity to explain its high electrical conductivity and inferred high Poisson's ratio.

Downdip rupture limit from the updip limit of seismic tremor and slow slip (ETS)

Another indicator of the downdip limit of megathrust rup-

Fig. 14. Compilation of Cascadia coseismic coastal subsidence data for the 1700 (dark band) and earlier great events (light band) compared with (*a*) the predictions for 500–800 years of strain build up and (*b*) for 10–50 m of rupture displacement (after Leonard et al. 2010).

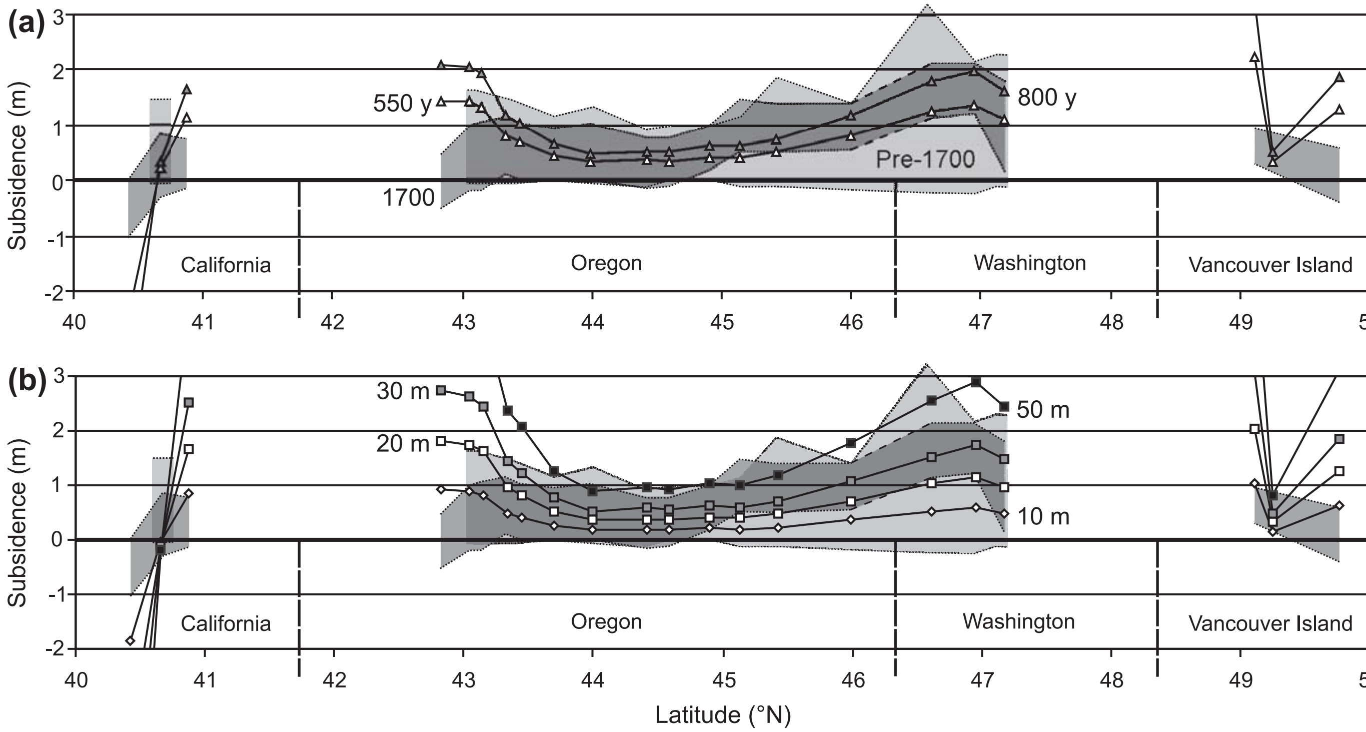

ture is the updip limit of episodic tremor and slip discussed in the next section. Since most, if not all, of the plate convergence is accounted for in slow slip events (e.g., Dragert et al. 2004; Chapman and Melbourne 2009), there can be little elastic strain build up at the depths of ETS for subsequent earthquake rupture. The tremor locations are difficult to determine accurately because they have no clear phase onsets. However, they have been studied in detail and are quite well located, although scattered (e.g., Kao et al. 2009, and references therein). The slow slip events are less well located since the locations depend on matching the surface displacements to dislocation models and are sensitive to the assumed thrust fault depth profile. However, the seaward slow slip limit must be quite close to that of the tremor. The ETS tremor intensity and modelled slow slip taper seaward and the locked fault geodetic model and thermal rupture limit models taper landward (Figs. 12, 13), but there may be a gap between them (e.g., Dragert et al. 2004; Chapman and Melbourne 2009). In any case, the seaward ETS limits are approximately parallel to the downdip seismogenic limits so, with a possible as yet poorly calibrated downdip offset, the ETS distribution may provide an important landward rupture constraint.

Episodic tremor and slip

The recent discovery of episodic tremor and slip (Rogers and Dragert 2003; Kao et al. 2009) has added to our understanding of the subduction seismic and aseismic slip process in the Cascadia subduction zone. Similar ETS has been observed on the margin of southwest Japan (e.g., Obara 2002) and a few other subduction zones. These recurring events (Fig. 15) mainly appear to be limited to subduction zones with oceanic lithosphere ages of up to a few tens of millions of years, although the required careful monitoring is available only for a few subduction zones globally. The association with young ages suggests that only the warmer subduction zones have ETS. It appears that most of the time the subduction interface is locked to a considerable distance downdip of the megathrust rupture zone. This short-term locking extends updip to about the west coast of Vancouver Island and includes a zone where the temperatures are higher than for normal brittle seismic behaviour. The strength of the fault on the downdip portion is exceeded after about a year (about 14 to 15 months in the case of the southern Vancouver Island segment), and it fails in a slow slip process. The slip propagates along strike at a rate of up to 10 km/day, and it takes the order of two weeks to complete a typical event. These ETS events are detected in two ways, geodetically by a reversal in the direction of continuous GPS installations in the coastal region, and by the onset of almost continuous pulsating sequences of non-earthquake seismic signals called "tremor." They consist of multiple overlapping bursts of shear-wave energy that, unlike earthquakes, have no sharp phase onset. During the entire rupture episode there are tremor sequences that have durations of minutes to hours (e.g., Kao et al. 2009, and references therein). Some smaller tremor sequences, and probably accompanying slip, occur between the main ETS events (e.g., Fig. 15; Creager 2009; Kao et al. 2009). Beneath Vancouver Island the tremors are mainly concentrated at the depth of the Lithoprobe "E" layer (Fig. 16*a*), where the underlying "F" layer, interpreted to be the top of the oceanic plate, is at depths of 30–50 km (Fig. 16*b*).

Fig. 15. Correspondence of slow slip events detected by GPS and tremor events detected by seismographs at Victoria, B.C. (Updated from Rogers and Dragert 2003).

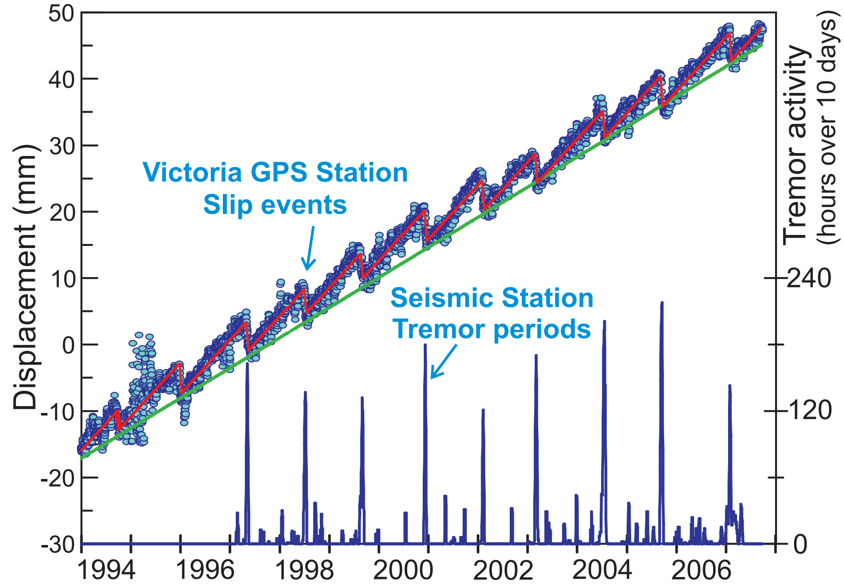

Fig. 16. (*a*) Colour contours of tremor intensity in the area of the Lithoprobe corridor (after Kao et al. 2009). Tremors are concentrated near the depth of the E-layer reflective band and receiver function low-velocity zone. (*b*) Map of tremor activity locations 1997–2007 (after Kao et al. 2009). Tremor appears to avoid area of two large crustal earthquakes on Vancouver Island. ETS, episodic tremor and slip.

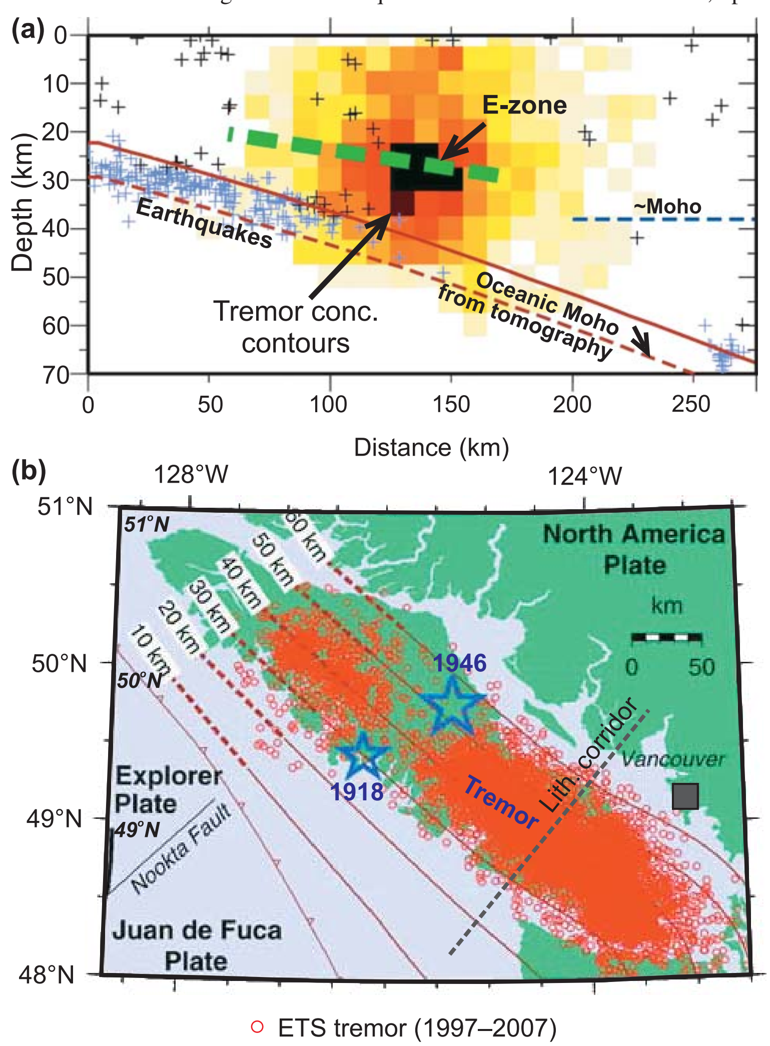

In the ETS process, the stress that had accumulated on the deeper slow slip portion of the fault is transferred to the upper more strongly locked portion that will eventually fail in a great subduction earthquake (Dragert et al. 2004). Because the stress is accumulated incrementally rather than continuously, it is expected that the subduction zone will preferentially fail during one of these incremental increases in stress (Dragert et al. 2001; Mazzotti and Adams 2004). However, it is now recognized that different portions of the Cascadia subduction zone have slow slip events at different times and have different return periods (e.g., Brudzinski and Allen 2007), so we cannot yet use the ETS events to usefully estimate time variations in Cascadia great earthquake rupture probability.

A number of observations provide constraints to the process responsible for ETS. One constraint on the nature of the ETS process in the Cascadia Subduction Zone is provided by frequently repeated high-precision absolution gravity measurements (Lambert et al. 2006). The ETS events are accompanied by gravity changes that are most likely caused by mass redistribution and not height change. Another important observation is that ETS activity appears to be modulated by earth tides (Rubinstein et al. 2008; Lambert et al. 2009). Concentrations of tremor activity are observed with periods of 12.4 and 24–25 h, the same as the principal lunar and lunisolar tides. This indicates that the small stresses associated with the solid-earth and ocean tides influence the genesis of tremor much more effectively than they do the genesis of normal earthquakes. Because the lithostatic stresses are 10^5 times larger than those associated with the tides, it is argued that tremor occurs on very weak faults (e.g., Rubinstein et al. 2008). Slip may be mediated by pressure fluctuations of fluids rising from the subducting slab. Julian (2002) and others have argued that the fluids come from especially strong dehydration of the downgoing slab beneath the fore-arc region in hot subduction zones, as for example shown by Peacock and Wang (1999).

The great earthquake hazard

A detailed discussion of the hazard associated with great subduction zone earthquakes in Cascadia is beyond the scope of this article, but we present here a few general comments. Different locations across the margin will have different experiences. The outer coast, which is approximately above the down-dip limit of the earthquake rupture, will be subject to strong shaking, which is likely to damage many structures, trigger landslides, and cause liquefaction in susceptible regions. The outer coast also will be subject to abrupt subsidence of 0.5–2 m and to very large tsunami waves. The major urban regions of Cascadia are at a distance inland such that the shaking is not as severe as on the outer coast. However, the long duration of several minutes of shaking may trigger landslides and make some structures vulnerable, structures that would not be seriously affected by stronger shaking with a shorter duration. Because of attenuation with distance of high-frequency waves, longer period waves become dominant at landward locations. Some structures may be especially vulnerable to such waves.

Great progress has been made in understanding the hazard from great subduction earthquakes since the first Lithoprobe studies on Vancouver Island. Scenario development (e.g., Cascadia Regional Earthquake Work Group 2005) using information from other great earthquakes, such as Sumatra (2004) and Alaska (1964), has facilitated detailed planning by emergency organizations. The hazard from great subduction earthquakes is now included in the latest editions of building codes in both Canada (e.g., Adams and Atkinson 2003) and the USA (e.g., Petersen et al. 2008).

The attenuation of shaking with distance relationships currently used in Cascadia hazard assessments depend mainly on strong motion shaking recorded from great earthquakes in other subduction zones (e.g., Atkinson and Macias 2009; Gregor et al. 2002). More accurate estimates of the attenuation with distance specifically for Cascadia are needed and structural studies, such as Lithoprobe pioneered, can provide new constraints. Such studies are likely to play an increasing role in the next generation of seismic hazard assessments. Detailed knowledge of the structure in the subduction region coupled with wave amplitude modelling can identify regions that are subject to especially high shaking. Examples of possible causes of high amplitudes are where there is focusing by low-velocity fore-arc mantle serpentinized regions (McNeill et al. 2004), sub-critical reflections off the Moho of the subducting plate (Cohee et al. 1991; McNeill 2005), and the effects of sedimentary basin response (e.g., Olsen et al. 2008). The earthquake threat for the coastal region of British Columbia and Washington is large even without great earthquakes. The evidence for giant subduction zone events results in hazard estimates that are similar to regions well known for substantial earthquake hazard, such as California and Japan.

Acknowledgements

We acknowledge the many colleagues and collaborators at the Pacific Geoscience Centre, Geological Survey of Canada, and the US Geological Survey; the universities of Victoria, British Columbia, Simon Fraser, and Washington; and many others elsewhere that have contributed to the work leading to our improved understanding of the great earthquake process on the coast of Vancouver Island and the rest of Cascadia. We especially acknowledge the Lithoprobe program and its Director Ron Clowes for the large contributions to the subject through that program; he is also guest editor of this volume and provided important review comments. We acknowledge very helpful formal reviews by K. Creager and I. Hutchinson, and informal reviews by H. Dragert and A. Calvert that substantially improved the manuscript.

References

Adams, J. 1990. Paleoseismicity of the Cascadia subduction zone: Evidence from turbidites off the Oregon–Washington margin. Tectonics, **9**: 569–583.

Adams, J., and Atkinson, G. 2003. Development of seismic hazard maps for the proposed 2005 edition of the National Building Code of Canada. Canadian Journal of Civil Engineering, **30**: 255–271. doi:10.1139/l02-070.

Ando, M. 1975. Source mechanisms and tectonic significance of historical earthquakes along the Nankai Trough. Tectonophysics, **27**: 119–140.

Arima, E.Y., St. Claire, E., Clamhouse, L., Edgar, J., Jones, C., and Thomas, J. 1991. Between Ports Alberni and Renfrew: Notes on west coast peoples. Canadian Museum of Civilization. Canadian Ethnology Service, Mercury Series Paper 121, 323 p.

Atkinson, G.M., and Macias, M. 2009. Predicted ground motions for great interface earthquakes in the Cascadia subduction zone. Bulletin of the Seismological Society of America, **99**: 1552–1578. doi:10.1785/0120080147.

Atwater, B.F. 1987. Evidence for great Holocene earthquakes along the outer coast of Washington state. Science, **236**: 942–944.

Atwater, B.F. 1992. Geologic evidence for earthquakes during the past 2000 years along the Copalis River, southern coastal Washington. Journal of Geophysical Research, **97**: 1901–1919.

Atwater, B.F., and Hemphill-Haley, E. 1997. Recurrence intervals for great earthquakes of the past 3500 years at northeastern Willapa Bay. US. Geological Survey, Professional Paper 1576, 108 p.

Atwater, B.F., Nelson, A.R., Clague, J.J., Carver, G.A., Yamaguchi, D.K., Bobrowsky, P.T., et al. 1995. Summary of coastal geologic evidence for past great earthquakes at the Cascadia subduction zone. Earthquake Spectra, **11**: 1–18.

Atwater, B.F., Musumi-Rokkaku, S., Satake, K., Tsuji, Y., Ueda, K., and Yamaguchi, D.K. 2005. The orphan tsunami of 1700; Japanese clues to a parent earthquake in North America. US. Geological Survey, Professional Paper 1707, published in association with University of Washington Press, Seattle, Wash.

Audet, P., Bostock, M.G., Mercier, J.-P., and Cassidy, J.F. 2008. Morphology of the Explorer – Juan de Fuca slab edge in northern Cascadia: Imaging plate capture at the ridge–trench transform triple junction. Geology, **36**: 895–898. doi:10.1130/G25356A.1.

Audet, P., Bostock, M.G., Christensen, N.I., and Peacock, S.M. 2009. Seismic evidence for overpressured subducted oceanic crust and megathrust fault sealing. Nature, **457**: 76–78. doi:10.1038/nature07650.

Benson, B.E., Clague, J.J., and Grimm, K. 1999. Relative sea-level change inferred from intertidal sediments beneath marshes on Vancouver Island, British Columbia. Quaternary International, **60**: 49–54. doi:10.1016/S1040-6182(99)00006-3.

Blais-Stevens, A., Rogers, G.C., and Clague, J.J. 2009. A 4000-year record of earthquakes in late hlocene sediments from Saanich Inlet, an anoxic fiord near Victoria, British Columbia. Seismological Research Letters, **80**: 294.

Brocher, T.M., T. Parsons, R.E. Blakely, N.I. Christensen, M.A. Fisher, R.E. Wells, and the SHIPS Working Group(12 authors). 2001. Three-dimensional geometry of crustal faults, basins, and uplifts in Puget Lowland, Washington: Results from SHIPS, the 1998 seismic hazards investigation in Puget Sound. Journal of Geophysical Research, **106**: 13 541 – 13 564.

Brudzinski, M.R., and Allen, R.M. 2007. Segmentation in episodic tremor and slip all along Cascadia. Geology, **35**: 907–910. doi:10.1130/G23740A.1.

Calvert, A.J. 1996. Seismic reflection constraints on imbrication and underplating of the northern Cascadia convergent margin. Canadian Journal of Earth Sciences, **33**: 1294–1307. doi:10.1139/e96-098.

Calvert, A.J. 2004. Seismic reflection imaging of two megathrust shear zones in the northern Cascadia subduction zone. Nature, **428**: 163–167. doi:10.1038/nature02372.

Calvert, A.J., and Clowes, R.M. 1990. Deep, high amplitude reflections from a major shear zone above the subducting Juan de Fuca plate. Geology, **18**: 1091–1094.

Calvert, A.J., Fisher, M.A., Ramachandran, K., and Trehu, A.M. 2003. Possible emplacement of crustal rocks into the forearc mantle of the Cascadia subduction zone. Geophysical Research Letters, **30**: doi:10.1029/2003GL018541.

Cascadia Regional Earthquake Work Group. 2005. Cascadia subduction zone earthquakes: a magnitude 9.0 earthquake scenario. Oregon Department of Geology and Mineral Industries, Open File O-05-05.

Cassidy, J.F., and Ellis, R.M. 1993. *S*-wave velocity structure of the Northern Cascadia subduction zone. Journal of Geophysical Research, **96**(B12): 19 843 – 19 851.

Cassidy, J.F., and Waldhauser, F. 2003. Evidence for both crustal and mantle earthquakes in the subducting Juan de Fuca plate. Geophysical Research Letters, **30**: . doi:10.1029/2002GL015511.

Cassidy, J.F., Ellis, R.M., and Rogers, G.C. 1988. The 1918 and 1957 Vancouver Island earthquakes. Bulletin of the Seismological Society of America, **78**: 617–635.

Cassidy, J.F., Rogers, G.C., and Hyndman, R.D. 2003. The Pacific Geoscience Centre and one hundred years of seismological studies on Canada's west coast. *In* International handbook of earthquake and engineering seismology. *Edited by* W.H.K. Lee, H. Kanamori, P. Jennings, and C. Kisslinger. Academic Press, Chap. 79.12, part B.

Chapman, J.S., and Melbourne, T.I. 2009. Future Cascadia megathrust rupture delineated by episodic tremor and slip. Geophysical Research Letters, **36**: L22301. doi:10.1029/2009GL040465.

Cherniawsky, J.Y., Titov, V.V., Wang, K., and Li, J.-Y. 2007. Numerical simulations of tsunami waves and currents for southern Vancouver Island from a Cascadia megathrust earthquake. Pure and Applied Geophysics, **164**: 465–492. doi:10.1007/s00024-006-0169-0.

Clague, J.J. 1995. Early historical and ethnographical accounts of large earthquakes and tsunamis on western Vancouver Island, British Columbia. *In* Current research. Geological Survey of Canada, Paper 1995-A, pp. 47–50.

Clague, J.J., and Bobrowsky, P.T. 1994*a*. Evidence for a large earthquake and tsunami 100–400 years ago on western Vancouver Island, British Columbia. Quaternary Research, **41**: 176–184.

Clague, J.J., and Bobrowsky, P.T. 1994*b*. Tsunami deposits in tidal marshes on Vancouver Island, British Columbia. Geological Society of America Bulletin, **106**: 1293–1303.

Clague, J.J., and Bobrowsky, P.T. 1999. The geological signature of great earthquakes off Canada's west coast. Geoscience Canada, **26**: 1–15.

Clague, J.J., Bobrowsky, P., and Hyndman, R.D. 1995. The great earthquake threat in southwestern British Columbia. The B.C. Professional Engineer, **46**: 4–8.

Clague, J.J., Bobrowsky, P.T., and Hutchinson, I. 2000. A review of geological records of large tsunamis at Vancouver Island, British Columbia, and implications for hazard. Quaternary Science Reviews, **19**: 849–863.

Clowes, R.M., and Hyndman, R.D. 2002. Geophysical studies of the northern Cascadia subduction zone off western Canada and their implications for great earthquake seismotectonics: A review. *In* Seismotectonics at the subduction zone. *Edited by* Y. Fujinawa. Terra Scientific Publishing, Tokyo, Japan, pp. 1–23.

Clowes, R.M., Brandon, M.T., Green, A.G., Yorath, C.J., Sutherland Brown, A., Kanesewich, E.R., and Spencer, C. 1987*a*. Lithoprobe — southern Vancouver Island: Cenozoic subduction complex imaged by deep seismic reflections. Canadian Journal of Earth Sciences, **24**: 31–51.

Clowes, R.M., Yorath, C.J., and Hyndman, R.D. 1987*b*. Reflection mapping across the convergent margin of western Canada. Geophysical Journal of the Royal Astronomical Society, **89**: 79–84.

Cohee, B.P., Somerville, P.G., and Abrahamson, N.A. 1991. Simulated ground motions for hypothesized Mw 8 subduction earthquakes in Washington and Oregon. Bulletin of the Seismological Society of America, **81**: 28–56.

Creager, K. 2009. Tremors between slip events: more evidence of great quake danger to Seattle. Science Daily News, Dec. 16, 2009.

Currie, C.A., Hyndman, R.D., Wang, K., and Kostoglodov, V.

2002. Thermal models of the Mexico subduction zone: Implications for the megathrust seismogenic zone. Journal of Geophysical Research, **107**: doi:10.1029/2001JB000886.

Currie, C.A., Wang, K., Hyndman, R.D., and He, J. 2004. The thermal effects of slab-driven mantle flow above a subducting plate: The Cascadia subduction zone and backarc. Earth and Planetary Science Letters, **223**: 35–48.

Dallimore, A., Enkin, R.J., Baker, J., and Rogers, G.C. 2009. Identification and frequency of Holocene earthquakes from the laminated sedimentary record of Effingham Inlet, Pacific coast Vancouver Island, British Columbia.. Seismological Research Letters (Abstracts), **80**: 322.

Davis, E.E., and Hyndman, R.D. 1989. Accretion and recent deformation of sediments along the northern Cascadia subduction zone. Geological Society of America Bulletin, **101**: 1465–1480.

Dragert, H., and Hyndman, R.D. 1995. Continuous GPS monitoring of elastic strain in the northern Cascadia subduction zone. Geophysical Research Letters, **22**: 755–758.

Dragert, H., Hyndman, R.D., Rogers, G.C., and Wang, K. 1994. Current deformation and the width of the seismogenic zone of the northern Cascadia subduction thrust. Journal of Geophysical Research, **99**: 653–668.

Dragert, H., Wang, K., and James, T.S. 2001. A silent slip event on the deeper Cascadia subduction interface. Science, **292**: 1525–1528.

Dragert, H., Wang, K., and Rogers, G. 2004. Geodetic and seismic signatures of episodic tremor and slip in the northern Cascadia subduction zone. Earth and Planetary Science Letters, **56**: 1143–1150.

Fisher, M.A., Parsons, T., and Brocher, T.M. 1999. Seismic survey probes urban earthquake hazard in Pacific Northwest. EOS, Transactions of the American Geophysical Union, **80**(2): 13–17.

Flück, P., Hyndman, R.D., and Wang, K. 1997. Three-dimensional dislocation model for great earthquakes of the Cascadia subduction zone. Journal of Geophysical Research, **102**: 20 539 – 20 550.

Geist, E.L. 1999. Local tsunamis and earthquake source parameters. Advances in Geophysics, **39**: 117–209.

Geist, E.L. 2005. Local Tsunami Hazards in the Pacific Northwest from Cascadia Subduction Zone Earthquakes. US. Geological Survey, Professional Paper 1661B, 17 p.

Geist, E., and Yoshioka, S. 1996. Source parameters controlling the generation and propagation of potential local tsunamis along the Cascadia margin. Natural Hazards, **13**: 151–177.

Goldfinger, C., Nelson, C.H., and Johnson, J.E. 2003. Holocene earthquake records from the Cascadia subduction zone and northern San Andreas fault based on precise dating of offshore turbidites. Annual Review of Earth and Planetary Sciences, **31**: 555–577.

Goldfinger, C., Nelson, C.H., Johnson, J.E., Morey, A.E., Gutiérrez-Pastor, J., Karabanov, E., et al., and the Shipboard Scientific Parties. 2009. Turbidite event history: methods and implications for Holocene paleoseismicity of the Cascadia subduction zone: US. Geological Survey, Professional Paper 1661-F.

Graindorge, D., Spence, G., Charvis, P., Collot, J.Y., Hyndman, R.D., and Trehu, A.M. 2003. Crustal structure beneath the Strait of Juan de Fuca and southern Vancouver Island from seismic and gravity analyses. Journal of Geophysical Research, **108**. doi:10.1029/2002JB001823.

Green, A.G., Clowes, R.M., Yorath, C.J., Spencer, C., Kanasewich, E.R., Brandon, M.T., and Sutherland Brown, A. 1986. Seismic reflection imaging of the subducting Juan de Fuca plate. Nature, **319**: 210–213.

Gregor, N., Silva, W., Wong, I., and Youngs, R. 2002. Ground-motion attenuation relationships for Cascadia subduction zone megathrust earthquakes based on a stochastic finite-fault model. Bulletin of the Seismological Society of America, **92**: 1923–1932.

Griggs, G.B., and Kulm, L.D. 1970. Sedimentation in Cascadia deep-sea channel. Geological Society of America Bulletin, **81**: 1361–1384.

Guilbault, J.P., Clague, J.J., and Lapointe, M. 1996. Foraminifera evidence for the amount of coseismic subsidence during a late Holocene earthquake on Vancouver Island, west coast of Canada. Quaternary Science Reviews, **15**: 913–937.

Gutenberg, B., and Richter, C.F. 1954. Seismicity of the Earth and associated phenomena. Princeton University Press, Princeton, N.J.

Harris, R.N., and Wang, K. 2007. Thermal models of the Middle America trench at the Nicoya Peninsula. Costa Rica. Geophysical Research Letters, **29**: . doi:10.1029/2002GL015406.

Heaton, T.H., and Hartzell, S.H. 1986. Source characteristics of hypothetical subduction earthquakes in the northwestern United States. Bulletin of the Seismological Society of America, **76**: 675–708.

Heaton, T.H., and Hartzell, S.H. 1987. Earthquake hazards on the Cascadia subduction zone. Science, **236**: 162–168.

Heaton, T.H., and Kanamori, H. 1984. Seismic potential associated with subduction in the northwestern United States. Bulletin of the Seismological Society of America, **74**: 933–944.

Heaton, T.H., and Snavely, P.D. 1985. Possible tsunami along the northwestern coast of the United States inferred from Indian traditions. Seismological Society of America Bulletin, **75**: 1455–1460.

Hippchen, S., and Hyndman, R.D. 2008. Thermal and Structural Models of the Sumatra Subduction Zone: Implications for the Megathrust Seismogenic Zone. Journal of Geophysical Research, **113**. doi:10.1029/2008JB005698.

Hu, Y., Wang, K., He, J., Klotz, J., and Khazaradze, G. 2004. Three-dimensional viscoelastic finite element model for post-seismic deformation of the great 1960 Chile earthquake. Journal of Geophysical Research, **109**. doi:10.1029/2004JB003163.

Hyndman, R.D. 1988. Dipping seismic reflectors, electrically conductive zones, and trapped water in the crust over a subducting plate. Journal of Geophysical Research, **93**: 13 391 – 13 405.

Hyndman, R.D. 1995*a*. Great earthquakes in the Pacific Northwest. Scientific American, **273**: 50–57.

Hyndman, R.D. 1995*b*. The Lithoprobe corridor across the Vancouver Island continental margin: the structural and tectonic consequences of subduction. Canadian Journal of Earth Sciences, **32**: 1777–1802.

Hyndman, R.D. 2007. The seismogenic zone of subduction thrust faults: What we know and don't know. *In* The seismogenic zone of subduction thrust faults, *Edited by* T.H. Dixon and J.C. Moore. Columbia University Press, New York, N.Y., pp. 15–40.

Hyndman, R.D., and Peacock, S.M. 2003. Serpentinization of the forearc mantle. Earth and Planetary Science Letters, **212**: 417–432.

Hyndman, R.D., and Wang, K. 1993. Thermal constraints on the zone of major thrust earthquake failure: The Cascadia subduction zone. Journal of Geophysical Research, **98**: 2039–2060.

Hyndman, R.D., and Wang, K. 1995. Constraints on the rupture zone of great earthquakes on the Cascadia subduction thrust from current deformation and the thermal regime. Journal of Geophysical Research, **98**: 2039–2060.

Hyndman, R.D., Yorath, C.J., Clowes, R.M., and Davis, E.E. 1990. The northern Cascadia subduction zone at Vancouver Island: seismic structure and tectonic history. Canadian Journal of Earth Sciences, **27**: 313–329.

Hyndman, R.D., Wang, K., and Yamano, M. 1995. Thermal constraints on the seismogenic portion of the southwestern Japan subduction zone. Journal of Geophysical Research, **100**: 15 373 – 15 392.

Hyndman, R.D., Rogers, G.C., Dragert, H., Clague, J.J., Adams, J., and Bobrowsky, P.T. 1996. Giant earthquakes beneath Canada's west coast. Geoscience Canada, **23**: 63–72.

Jacoby, G.C. 1995. Tree-ring applications to paleoseismicity studies. Pacific Northwest, Geological Association of Canada, Annual Meeting, Victoria, B.C., May 17–19, 1995. Geological Association of Canada, Program with Abstracts, **20**: A-117.

Julian, B. 2002. Seismological Detection of Slab Metamorphism. Science, **296**: 1625–1626.

Kao, H., Shan, S.-J., Dragert, H., and Rogers, G. 2009. Northern Cascadia episodic tremor and slip: A decade of tremor observations from 1997 to 2007. Journal of Geophysical Research, **114**: B00A12. doi:10.1029/2008JB006046.

Kroeber, A.L. 1976. Yurok Myths. University of California Press, Berkeley, Calif.

Kummer, T., and Spinelli, G.A. 2009. Thermal effects of fluid circulation in the basement aquifer of subducting ocean crust. Journal of Geophysical Research, **114**: B03104. doi:10.1029/2008JB006197.

Kurtz, R.D., DeLaurier, J.M., and Gupta, J.C. 1986. A magnetotelluric sounding across the subducting Juan de Fuca plate. Nature, **321**: 596–599.

Lambert, A., Courtier, N., and James, T.S. 2006. Long-term monitoring by absolute gravimetry: Tides to postglacial rebound. Journal of Geodynamics, **41**: 307–317.

Lambert, A., Kao, H., Rogers, G.C., and Courtier, N. 2009. Correction to "Correlation of tremor activity with tidal stress in the northern Cascadia subduction zone". Journal of Geophysical Research, **114**: B00A99. doi:10.1029/2008JB006887.

Leonard, L.J., Hyndman, R.D., and Mazzotti, S. 2004. Coseismic subsidence in the 1700 great Cascadia earthquake: Coastal estimates versus elastic dislocation models. Geological Society of America Bulletin, **116**. doi:10.1130/B25369.2.

Leonard, L.J., Currie, C.A., Mazzotti, S., and Hyndman, R.D. 2010. Rupture area and displacement of past Cascadia great earthquakes from coastal coseismic subsidence. Geological Society of America Bulletin, In press.

Lewis, T.J., Bentkowski, W.H., Davis, E.E., Hyndman, R.D., Souther, J.G., and Wright, J.A. 1988. Subduction of the Juan de Fuca Plate: thermal consequences. Journal of Geophysical Research, **93**: 15 207 – 15 225.

Ludwin, R.S., Dennis, R., Carver, D., McMillan, A.D., Losey, R., Clague, J., et al. 2005. Dating the 1700 Cascadia Earthquake — Great Coastal Earthquakes in Native Stories. Seismological Research Letters, **76**: 140–148.

Mazzotti, S., and Adams, J. 2004. Variability of Near-Term Probability for the Next Great Earthquake on the Cascadia Subduction Zone. Bulletin of the Seismological Society of America, **94**: 1954–1959. doi:10.1785/012004032.

Mazzotti, S., Dragert, H., Henton, J., Schmidt, M., Hyndman, R., James, T., Lu, Y., and Craymer, M. 2003. Current tectonics of northern Cascadia from a decade of GPS measurements. Journal of Geophysical Research, **108**. doi:10.1029/2003JB002653.

McCaffrey, R., and Goldfinger, C. 1995. Forearc deformation and great subduction earthquakes: Implications for Cascadia offshore earthquake potential. Science, **267**: 856–859.

McCaffrey, R., Long, M.D., Goldfinger, C., Zwick, P.C., Nabelek, J.L., Johson, C.K., and Smith, C. 2000. Rotation and plate locking at the southern Cascadia subduction zone. Geophysical Research Letters, **27**: 3117–3120.

McCaffrey, R., Qamar, A.I., King, R.W., Wells, R., Khazaradze, G., Williams, C.A., et al. 2007. Fault locking, block rotation and crustal deformation in the Pacific Northwest. Geophysical Journal International, **169**: 1315–1340.

McCrory, P.A., Blair, J.L., Oppenheimer, D.H., and Walter, S.R. 2006. Depth to the Juan De Fuca slab beneath the Cascadia subduction margin — A 3-D model for sorting earthquakes. US. Geological Survey, Data Series 91, Version 1.2, 13 p.

McNeill, A.F. 2005. Contribution of post-critical reflections to ground motions from mega-thrust events in the Cascadia subduction zone. M.Sc. thesis, University of Victoria, Victoria, B.C., 180 p.

McNeill, A.F., Bostock, M.G., Rogers, G.C., and Shragge, J.C. 2004. The effect of forearc mantle serpentinization on ground motions from megathrust and intraslab events in the Cascadia Subduction Zone. Bulletin of the Seismological Society of America, **94**: 147–154.

Miller, M.M., Johnson, D.J., Rubin, C.M., Dragert, H., Wang, K., Qamar, A., and Goldfinger, C. 2001. GPS determination of along-strike variation in Cascadia margin kinematics: implications for relative plate motion, subduction zone coupling, and permanent deformation. Tectonics, **20**: 161–176.

Milne, W.G., Rogers, G.C., Riddihough, R.P., McMechan, G.A., and Hyndman, R.D. 1978. Seismicity of western Canada. Canadian Journal of Earth Sciences, **15**: 1170–1193.

Mitchell, C.E., Vincent, P., Weldon, R.J., and Richards, M.A. 1994. Present day vertical deformation of the Cascadia margin, Pacific Northwest, United States. Journal of Geophysical Research, **99**(B6): 12 257 – 12 277.

Murray, M., and Lisowski, M. 2000. Strain accumulation along the Cascadia subduction zone: Cape Mendocino to the Straits of Juan de Fuca. Geophysical Research Letters, **27**: 3631–3634.

Nedimovic, M.R., Hyndman, R.D., Ramachandran, K., and Spence, G.D. 2003. Reflection signature of seismic and aseismic slip on the northern Cascadia subduction interface. Nature, **24**: 416–420.

Nelson, A.R., Atwater, B.F., Bobrowsky, P.T., Bradley, L.-A., Clague, J.J., Carver, G.A., et al. 1995. Radiocarbon evidence for extensive plate-boundary rupture about 300 years ago at the Cascadia subduction zone. Nature, **378**: 371–374.

Nelson, A.R., Kelsey, H.M., and Witter, R.C. 2006. Great earthquakes of variable magnitude at the Cascadia subduction zone. Quaternary Research, **65**: 354–365.

Nicholson, T., Bostock, M., and Cassidy, J.F. 2005. New constraints on subduction zone structure in northern Cascadia. Geophysical Journal International, **161**: 849–859.

Obara, K. 2002. Nonvolcanic deep tremor associated with subduction in southwest Japan. Science, **296**: 1679–1681.

Oleskevich, D.A., Hyndman, R.D., and Wang, K. 1999. The updip and downdip limits to great subduction earthquakes: Thermal and structural models of Cascadia, south Alaska, SW Japan, and Chile. Journal of Geophysical Research, **104**: 14 965 – 14 992.

Olsen, K.B., Stephenson, W.J., and Geisselmeyer, A. 2008. 3D crustal structure and long- period ground motions from a M 9.0 megathrust earthquake in the Pacific Northwest region. Journal of Seismology, **12**: 145–151.

Oppenheimer, D.H., Eaton, J., Jayko, A., Lisowski, M., Marshall, G., Murray, M., et al. 1993. The Cape Mendocino, California, earthquakes of April 1992: Subduction at the Triple Junction. Science, **261**: 433–438.

Peacock, S.M., and Hyndman, R.D. 1999. Hydrous minerals in the mantle wedge and the maximum depth of subduction earthquakes. Geophysical Research Letters, **26**: 2517–2520.

Peacock, S.M., and Wang, K. 1999. Seismic consequences of warm versus cool subduction metamorphism: examples from southwest and northeast Japan. Science **286**: 937–939. doi:10.1126/science.286.5441.937..

Peters, R., Jaffe, B., Gelfenbaum, G., and Peterson, C. 2003. Cascadia tsunami deposit database: US. Geological Survey, Open-File Report 03-13, 24 p.

Petersen, M.D., Frankel, A.D., Harmsen, S.C., Mueller, C.S., Haller, K.M., Wheeler, R.L., et al. 2008. Documentation for the 2008 update of the United States national seismic hazard maps. US. Geological Survey, Open-File Report 2008-1128, 61 p.

Peterson, C.D., and Darienzo, M.E. 1991. Discrimination of climatic, oceanic and tectonic mechanisms of cyclic marsh burial from Alsea Bay, Oregon, U.S.A. US. Geological Survey, Open File Report 91-441-C, 53 p.

Preston, L.A., Creager, K.C., Crosson, R.S., Brocher, T.M., and Tréhu, A.M. 2003. Intraslab earthquakes: Dehydration of the Cascadia slab. Science, **302**: 1197–1200.

Priest, R.G., Myers, E., Baptista, A.M., Fleuck, P., Leuck, P., Wang, K., and Peterson, C.D. 2000. Source simulation for tsunamis: Lessons learned from fault rupture modeling of the Cascadia subduction zone, North America. Science of Tsunami Hazards, **18**: 77–106.

Ramachandran, K., Dosso, S.E., Spence, G.D., Hyndman, R.D., and Brocher, T.M. 2005. Forearc structure beneath southwestern British Columbia: A three-dimensional tomographic velocity model. Journal of Geophysical Research, **110**. doi:10.1029/2004JB003258.

Ramachandran, K., Hyndman, R.D., and Brocher, T.M. 2006. Regional *P* wave velocity structure of the northern Cascadia subduction zone. Journal of Geophysical Research, **111**. doi:10.1029/2005JB004108.

Reid, H.F. 1910. The Mechanics of the Earthquake. The California Earthquake of April 18, 1906. Carnegie Institution of Washington, Washington, D.C., Report of the State Investigation Commission, Vol. 2.

Reilinger, R., and Adams, J. 1982. Geodetic evidence for active landward tilting of the Oregon and Washington coastal ranges. Geophysical Research Letters, **9**: 401–403.

Riddihough, R.P. 1984. Recent movements of the Juan de Fuca plate system. Journal of Geophysical Research, **89**: 6980–6994.

Riddihough, R.P., and Hyndman, R.D. 1976. Canada's active western margin - the case for subduction. Geoscience Canada, **3**: 269–278.

Rogers, G.C. 1986. Seismic gaps along the Queen Charlotte Fault. Earthquake Prediction Research, **4**: 1–11.

Rogers, G.C. 1988. An assessment of the megathrust earthquake potential of the Cascadia subduction zone. Canadian Journal of Earth Sciences, **25**: 844–852.

Rogers, G.C. 1992. The history of earthquake studies in British Columbia, From Indian Legend to Satellite Technology. *In* Pioneering geology in the Canadian Cordillera. British Columbia Ministry of Energy, Mines and Petroleum Resources, Open File 1992-19.

Rogers, G.C. 1998. Earthquakes and earthquake hazard in the Vancouver area. *In* Geology and Natural Hazards of the Fraser River Delta, British Columbia. *Edited by* J.J. Clague, J.L. Luternauer, and D.C. Mosher. Geological Survey of Canada, Bulletin 525, pp. 17–25.

Rogers, G.C., and Crosson, R.S. 2002. Intraslab earthquakes beneath Georgia Strait/Puget Sound. *In* The Cascadia Subduction Zone and Related Subduction Systems — Seismic Structure, Intraslab Earthquakes and Processes, and Earthquake Hazards. *Edited by* S. Kirby, K. Wang, and S. Dunlop. US. Geological Survey, Open-File Report 02-328, and Geological Survey of Canada, Open File 4350.

Rogers, G., and Dragert, H. 2003. Episodic Tremor and Slip on the Cascadia Subduction Zone: The Chatter of Silent Slip. Science, **300**: 1942–1943.

Rogers, G.C., and Hasegawa, H.S. 1978. A second look at the British Columbia earthquake of June 23, 1946. Bulletin of the Seismological Society of America, **68**: 653–676.

Rogers, G.C., and Horner, R.B. 1991. An overview of western Canadian seismicity. *In* Neotectonics of North America. *Edited by* D.B. Slemmons, E.R. Engdahl, M.D. Zoback, and D.D. Blackwell. Geological Society of America, Geology of North America, Vol. 1, pp. 69–76.

Rogers, A.M., Walsh, T.J., Kockelman, W.J., and Priest, G.R. 1996. Earthquake hazards in the Pacific Northwest — an overview. US. Geological Survey, Professional Paper 1560, pp. 1–54.

Rubinstein, J.L., La Rocca, M., Vidale, J.E., Creager, K.C., and Wech, A.G. 2008. Tidal modulation of nonvolcanic tremor. Science, **319**: 186–189.

Satake, K., and Atwater, B.F. 2007. Long-term perspectives on giant earthquakes and tsunamis at subduction zones. Annual Review of Earth and Planetary Sciences, **35**: 349–374.

Satake, K., and Tanioka, Y. 1996. Tsunami heights along the Pacific Northwest computed from the M = 9 earthquake of January 1700. 92nd Annual Cordilleran Section. Geological Society of America, **28**(5): 108.

Satake, K., Shimazaki, K., Tsuji, Y., and Ueda, K. 1996. Time and size of a prehistoric great earthquake in the Cascadia subduction zone as inferred from Japanese tsunami records dated January 1700. Nature, **379**: 246–249.

Savage, J.C. 1983. A dislocation model of strain accumulation and release at a subduction zone. Journal of Geophysical Research, **88**: 4984–4996.

Savage, J.C., Lisowski, M., and Prescott, W.H. 1991. Strain accumulation in western Washington. Journal of Geophysical Research, **96**: 14 493 – 14 507.

Scholtz, C.H. 1990. Mechanics of Earthquakes and Faulting. Cambridge University Press, New York, N.Y., 439 p.

Shennan, I., and Hamilton, S. 2006. Coseismic and pre-seismic subsidence associated with great earthquakes in Alaska. Quaternary Science Reviews, **25**: 1–8.

Spence, G.D., Clowes, R.M., and Ellis, R.M. 1985. Seismic structure across the active subduction zone of western Canada. Journal of Geophysical Research, **90**: 6754–6772.

Spence, G.D., Hyndman, R.D., Lanton, S., Yorath, C.J., and Davis, E.E. 1991. Multi-channel seismic reflection profiles across the Vancouver Island continental shelf and slope. Geological Survey of Canada, Open File 2391.

Svarc, J.L., Savage, J.C., Prescott, W.H., and Murray, M.H. 2002. Strain accumulation and rotation in western Oregon and southwestern Washington. Journal of Geophysical Research, **107**: doi:10.1029/2001JB000625.

Tichelaar, B.W., and Ruff, L.J. 1993. Depth of seismic coupling along subduction zones. Journal of Geophysical Research, **98**: 2017–2037.

Tréhu, A.M., Braunmiller, J., and Nabelek, J.L. 2008. Probable low-angle thrust earthquakes on the Juan de Fuca – North America plate boundary. Geology, **36**: 127–130.

Underwood, M.B. 2007. Sediment inputs to subduction zones: Why lithostratigraphy and clay mineralogy matters. *In* The seismogenic zone of subduction thrust faults. *Edited by* T.H. Dixon and J.C. Moore. Columbia University Press, New York, N.Y., pp. 42–85.

Velasco, A.A., Ammon, C.J., and Lay, T. 1994. Recent large earthquakes near Cape Mendocino and in the Gorda plate: Broadband source time functions, fault orientations, and rupture complexities. Journal of Geophysical Research, **99**: 711–728.

von Huene, R., and Scholl, D.W. 1991. Observations at convergent margins concerning sediment subduction, subduction erosion, and the growth of continental crust. Reviews of Geophysics, **29**: 279–316.

Wang, K., and Rogers, G.C. 1994. An explanation for the double seismic layers north of the Mendocino triple junction. Geophysical Research Letters, **21**: 121–124.

Wang, K., Dragert, H., and Melosh, H.J. 1994. Finite element study of surface deformation in the northern Cascadia subduction zone. Canadian Journal of Earth Sciences, **31**: 1510–1522.

Wang, K., Wells, R., Mazzotti, S., Hyndman, R.D., and Sagiya, T. 2003. A revised dislocation model of interseismic deformation of the Cascadia subduction zone. Journal of Geophysical Research, **108**. doi:10.1029/2001JB001227.

Wilson, D.S. 1993. Confidence intervals for motion and deformation of the Juan de Fuca plate. Journal of Geophysical Research, **98**: 16 053 – 16 071.

Wolynec, L. 2000. Improving Model Constraints for Vertical Deformation Across the Northern Cascadia Margin. M.Sc. thesis, School of Earth and Ocean Sciences, University of Victoria, Victoria, B.C., Canada.

Yorath, C.J., Green, A.G., Clowes, R.M., Sutherland Brown, A., Brandon, M.T., Kanasewich, E.R., Hyndman, R.D., and Spencer, C. 1985. Lithoprobe, southern Vancouver Island: Seismic reflection sees through Wrangellia to the Juan de Fuca plate. Geology, **13**: 759–762.

Yorath, C.J., Sutherland Brown, A., and Massey, N.W.D. 1999. LITHOPROBE, southern Vancouver Island, British Columbia: geology. Geological Survey of Canada, Bulletin 498, 145 p.

Yoshioka, S., Wang, K., and Mazzotti, S. 2005. Interseismic locking of the plate interface in the northern Cascadia subduction zone, inferred from inversion of GPS data. Earth and Planetary Science Letters, **231**: 239–247.